

~~SECRET~~

Copy 10
RM SL54114



NACA

RESEARCH MEMORANDUM

for the

Atomic Energy Commission

AN INVESTIGATION OF THE LONGITUDINAL STABILITY
CHARACTERISTICS OF THREE SPECIALIZED STORE
CONFIGURATIONS AT TRANSONIC SPEEDS

By John A. Braden

Langley Aeronautical Laboratory
Langley Field, Va.

1. N. 17E-1372

Restriction/Classification
Cancelled

This material contains information of the espionage laws, Title 18 in any manner to an unauthorized person

United States within the meaning of the espionage laws, Title 18 or revelation of which in any manner to an unauthorized person

NATIONAL ADVISORY COMMITTEE
FOR AERONAUTICS
WASHINGTON

~~SECRET~~



NATIONAL ADVISORY COMMITTEE FOR AERONAUTICS

RESEARCH MEMORANDUM

for the
Atomic Energy Commission

AN INVESTIGATION OF THE LONGITUDINAL STABILITY
CHARACTERISTICS OF THREE SPECIALIZED STORE
CONFIGURATIONS AT TRANSONIC SPEEDS

By John A. Braden

SUMMARY

CLASSIFICATION CHANGED
 UNCLASSIFIED
 To
 By subject of CCN 212
 Mar. 31, 1954

Tests were conducted in the Langley 8-foot transonic pressure tunnel to determine the longitudinal stability characteristics of the TX-17, the "Short Seven," and the TX-21 special weapons. Dynamic and static stability data are presented over a Mach number range from about 0.50 to 1.20 for stagnation-pressure levels of about 0.6 and 1.0 atmosphere. The Reynolds number for the tests, based on maximum body diameter, varied for the individual models from about 1.0×10^6 to about 1.9 to 2.6×10^6 .

An investigation of the effects on longitudinal stability of a 0.007L nose extension to the TX-16 (TX-17) indicated that the nose extension was beneficial to the dynamic stability at the higher Mach numbers ($1.10 \leq M_0 \leq 1.20$) and produced minor reductions in the static stability through the Mach number range.

The Short Seven configuration was shown to have a relatively low level of dynamic and static stability up to $M_0 \approx 0.95$. At higher Mach numbers, the configuration was statically unstable.

Dynamic tests of the TX-21 showed that a change in the model nose contour from a two-radius-ogive flat to a hemispherical flat improved the dynamic-stability performance over most of the Mach number range, while the two-radius-ogive nose was beneficial to the static-stability characteristics for the same Mach numbers. A change in the TX-21 fin configuration from a 10° - 0° fin to a 6° - 14° double-wedge fin produced

~~SECRET~~
UNCLASSIFIED

~~RESTRICTED DATA~~
 THIS DOCUMENT CONTAINS RESTRICTED DATA AS DEFINED IN THE ATOMIC ENERGY ACT OF 1946. ITS TRANSMISSION OR DISCLOSURE OF ITS CONTENTS IN ANY MANNER TO AN UNAUTHORIZED PERSON IS PROHIBITED.

no appreciable changes in the level of $C_{m_q} + C_{m_{\dot{\alpha}}}$ but a definite increase (about 0.005) in the magnitude of $C_{m_{\alpha}}$ at most Mach numbers. An evaluation of the effects of spoiler-band addition and arrangement on the TX-21 showed that large improvements in both the dynamic and static-stability characteristics accompanied the addition of two spoiler bands to a clean configuration. Increasing the number of bands or judiciously rearranging the bands did not alter the dynamic-stability performance but improved the static stability. A forward movement in the center-of-gravity position, about 0.076L, for several configurations of the TX-21, was beneficial to both the dynamic and static-stability characteristics. An increase in the effective Reynolds number of a clean TX-21 configuration was accompanied by large reductions in the dynamic-stability performance and relatively smaller improvements in the static stability. No effect of Reynolds number was noted for banded configurations where the boundary layer was controlled primarily by the spoiler bands.

INTRODUCTION

Special weapons, released from high-altitude aircraft operating at Mach numbers near unity may attain supersonic speeds during their descent. Consequently, longitudinal stability problems associated with the transonic and supersonic speed ranges become of primary interest in the development of satisfactory aeroballistic shapes.

As a part of the special weapons program, the Atomic Energy Commission requested that tests be conducted in the Langley 8-foot transonic pressure tunnel on several specialized store configurations. In cooperation with the Sandia Corporation, investigations were made to determine the dynamic and static longitudinal stability performance of the TX-17, the "Short Seven," and the TX-21 special weapons. These tests were conducted in the Mach number range from about 0.50 to 1.20 at stagnation pressure levels of about 0.6 and 1.0 atmosphere.

Since this investigation constitutes only a portion of the overall performance analysis conducted under the special weapons program, any complete evaluation of these weapons, other than for the particular results obtained in the 8-foot transonic tunnel, will not be attempted.

SYMBOLS

M_0 free-stream Mach number
 V_0 free-stream velocity, ft/sec

- ρ_0 free-stream density, slugs/cu ft
- L body length, ft
- d maximum body diameter, ft
- S body frontal area, sq ft
- I transverse moment of inertia of the body about its center of gravity, slug-ft²
- $T_{1/2}$ time to damp to one-half amplitude for a decaying motion, sec
- T_2 time to increase to double amplitude for a divergent motion, sec
- P period of oscillation, sec
- α angle of attack, radians or deg
- q pitching velocity, radians/sec
- C_{m_q} effective rate of change of pitching-moment-curve slope with reduced pitching velocity, $\frac{\partial C_m}{\partial \left(\frac{qd}{2V} \right)} \Big|_{q \rightarrow 0}$
- $C_{m_{\dot{\alpha}}}$ effective rate of change of pitching-moment-curve slope with reduced rate of change of angle of attack, $\frac{\partial C_m}{\partial \left(\frac{\dot{\alpha}d}{2V} \right)} \Big|_{\dot{\alpha} \rightarrow 0}$
- $C_{m_q} + C_{m_{\dot{\alpha}}}$ rotational damping coefficient, per radian
- $C_{m_{\alpha}}$ static-longitudinal-stability parameter, $\partial C_m / \partial \alpha$, per deg

APPARATUS AND MODELS

Wind tunnel.- This investigation was conducted in the Langley 8-foot transonic tunnel, which permitted continuous testing up to a maximum Mach number of about 1.2 for these models. Details of the test-section geometry are given in reference 1. Tunnel calibrations have indicated that the flow angularity in the test section is about 0.1° downflow and that the maximum deviation from the average free-stream Mach number is about ± 0.004 at Mach numbers less than 1.00 and about ± 0.008 at supersonic conditions.

Model descriptions.- The three basic body shapes, provided by the Sandia Corporation, are designated herein as the TX-17, the Short Seven, and the TX-21. Coordinates for the TX-17 and Short Seven body contours are given in table I, while sketches of all the models, together with the model fins and other accessory parts are shown in figures 1 and 2.

The TX-17 model (fig. 1(a)) had a maximum diameter of 6.386 inches and represented the full-size weapon to 0.104 scale. This body was identical in external shape and dimensions to the TX-16 of reference 1 except for a 0.007L (0.208 in. model scale) extension to the nose which followed the existing TX-16 nose contour. Including this nose extension, the model had an overall length of 30.790 inches and a fineness ratio of 4.82. The TX-17 was tested with five spoiler bands, located as shown in figure 1(a), and four 6° - 14° double-wedge fins (fig. 1(b)) attached to the afterbody 45° from the vertical plane. The center of gravity was located at the 41.2 percent body station.

The Short Seven configuration (fig. 1(a)) had a maximum diameter of 7.500 inches and a model-to-prototype scale of 0.246. The overall body length was 21.88 inches while the fineness ratio was 2.92. Appendages tested with the Short Seven included two hemispherical antennae positioned in a horizontal plane on the nose flat, spoiler bands, and four 5° - 25° double-wedge stabilizing fins (fig. 1(b)). In addition, a drag plate of 32 percent porosity was attached to the model base (fig. 1(b)). The model center of gravity was located at the 39.3 percent body station.

Two basic configurations, to 0.116 scale, of the TX-21 were used in this investigation (fig. 2(a)). These models were tested with either a hemispherical-flat nose, designated as nose A, or a two-radius ogive flat nose, nose B, attached to a 6.5-inch (maximum diameter) cylindrical

afterbody. Cylindrical extensions of different lengths were interposed between the nose and afterbody to maintain an approximately constant model length. The overall length of the TX-21 with nose A was 16.756 inches whereas, the nose B configuration was 16.779 inches in length. The fineness ratio of both configurations was 2.58. The TX-21 models were tested with or without spoiler bands and with either the 6° - 14° double-wedge fins or the 10° - 0° fins. (See fig. 2(b).) All configurations of the TX-21 utilized the spoiler flange and the nut covers shown in figures 2(a) and 2(b), respectively. The normal centers of gravity for the nose A and B configurations were, respectively, at the 40.3 and 40.4 percent body stations.

All models were constructed principally of aluminum with the appendages and accessory parts screw-fastened to the body surfaces.

Dynamic rig.- A cutaway drawing of a typical test configuration mounted on the dynamic sting may be found in reference 1. The nose and afterbody sections were screw-fastened to the yoke of the dynamic rig and were statically balanced about the model pitch axis by means of steel counterweights. Changes in the model center-of-gravity position were made by a longitudinal shift of the model on the yoke. The models were actuated and controlled by hydraulic pistons for which a fluid pressure of 1,000 pounds per square inch was used. The attitude of the model was determined by the output of a bending beam instrumented with four strain gages.

TESTS AND METHODS

The Reynolds number for these tests (fig. 3), based on model maximum diameter, varied for the 6.5-inch models from about 1.0×10^6 to 1.4×10^6 at approximately 0.6 atmosphere and from approximately 1.5×10^6 to about 2.3×10^6 at 1.0 atmosphere. For the 7.5-inch model, the Reynolds number range was from about 1.9×10^6 to approximately 2.6×10^6 .

The nose flat of the TX-17 was positioned in the test section at about the 87-inch tunnel station, whereas, the nose flats of the TX-21 models and the Short Seven were located at about the 106-inch station. A typical test configuration mounted on the tunnel support system is shown schematically in figure 4.

For those conditions where the models were dynamically stable, dynamic and static stability records were obtained by deflecting the model from a stream alinement position to an angle of attack of about 9° and locking it in this deflected position. Upon release, the models oscillated with one degree of freedom. Three successive records of the time histories of these oscillatory motions were recorded on each of two types of instruments: a photographically recording galvanometer and a direct-inking oscillograph. In regions of dynamic instability, data were obtained by allowing the model to diverge from a stream-alinement position.

Previous investigations of similar models (refs. 1 and 2) have indicated that the natural frequency of the model on the support system was well in excess of the model frequencies encountered. Continuous monitoring of sting stresses during the stability investigations by means of electrical strain gages, attached at the intersection of the cylindrical and conical portions of the sting support, indicated negligible deflections of the support system under all loading conditions.

Tunnel stagnation pressures were manually recorded from an automatically compensating mercury-filled manometer. Flow visualization in the vicinity of the model was obtained through the use of standard schlieren photography.

REDUCTION OF DATA

The rotational damping coefficients $C_{m_q} + C_{m_{\dot{\alpha}}}$ and the static-longitudinal-stability parameter C_{m_α} were reduced as in references 1 and 2 according to the following equations:

$$-(C_{m_q} + C_{m_{\dot{\alpha}}}) = \frac{1.386}{T_{1/2}} \left(\frac{4I}{\rho_o V_o S d^2} \right)$$

$$(C_{m_q} + C_{m_{\dot{\alpha}}}) = \frac{1.386}{T_2} \left(\frac{4I}{\rho_o V_o S d^2} \right)$$

$$-C_{m_\alpha} = \frac{1.755I/d^3}{P^2 \rho_o V_o^2}$$

The time to damp to one-half amplitude $T_{1/2}$, or the time to double amplitude T_2 , and the period of the model motion P were obtained by averaging six successive oscillograph records taken at each test point with the two recording instruments. In regions where dynamic instability existed, the magnitude of the positive values of $C_{m_q} + C_{m_{\dot{\alpha}}}$ have not been presented because of the difficulty of obtaining accurate records in these regions. Static position calibrations were made at frequent intervals to determine the variation of the strain-gage output with model attitude. These calibrations proved to be sufficiently linear to permit the construction of the damping envelopes directly from the oscillograph records. For consistency, since the damping rate was nonlinear with amplitude, the damping envelope was constructed with the initial time at the beginning of the first cycle of model motion. This same time interval was included in the determination of the period of model motion P . Model moments of inertia were determined through the use of a calibrated torsional pendulum.

ACCURACY

In the reduction of the dynamic data, it was noted that changes in the rate of model damping $T_{1/2}$ at a test point, together with variations in the fairing of the damping envelope, could introduce random discrepancies between individual values of $T_{1/2}$ and the mean of six successive records of from 0 to 30 percent. While such discrepancies in the data do exist, it is believed that averaging the six successive records, for which a probable error in $C_{m_q} + C_{m_{\dot{\alpha}}}$ of ± 2 was computed, should give a reasonable degree of accuracy in magnitudes and should permit valid comparisons to be made between the various model configurations.

Excellent repeatability of the static-longitudinal-stability parameter $C_{m_{\dot{\alpha}}}$ was noted for all configurations and test conditions. The accuracy of $C_{m_{\dot{\alpha}}}$ is considered to be within 0.002. It should be noted that the magnitude of $C_{m_{\dot{\alpha}}}$ as obtained from dynamic tests represents an integrated average value between the oscillatory limits of the model and is correct or incorrect insofar as the actual slope of the moment curve is or is not linear.

It was shown in reference 2, in which the same dynamic sting was used, that neither strain-beam restoring moment or bearing frictional forces affected model damping significantly.

Schlieren studies of these tests have indicated that the body flow fields were influenced to an undetermined extent over a relatively small supersonic Mach number range by the reflection of the model bow wave from the tunnel walls. This Mach number range, which would contain spurious results in comparison to results in free air, would be primarily dependent upon the model length as well as the strength of the reflection. Examination of the model on the support system indicated the model center line to be $1\frac{5}{8}$ inches below the tunnel center line, so that the reflection struck the model after-body asymmetrically. The resulting differential pressures over the model were, in some cases, of sufficient intensity to create large angles of model trim. The Mach number range and the effects of this reflection on dynamic and static stability are discussed at greater length in the section entitled "RESULTS AND DISCUSSION."

RESULTS AND DISCUSSION

Tests of the TX-17 were made to determine the effects on longitudinal stability of a 0.208-inch nose extension to a particular configuration of the TX-16. While two configurations of the Short Seven were tested, longitudinal-stability data for only one configuration was obtained. For the TX-21, tests included the effects of modifications to the nose contour, fin shape, spoiler band arrangement, and center-of-gravity position on the longitudinal stability coefficients.

Data from the dynamic tests are presented as the variation of the rotational damping coefficient $C_{m_q} + C_{m_{\dot{\alpha}}}$ and the static-longitudinal-stability parameter $C_{m_{\alpha}}$ with Mach number. Data check points are indicated on the figures with flagged symbols.

Table II is presented as a summary of the major test results associated with the dynamic tests. Included in this table are the moments of inertia for each test configuration.

TX-17.- The effects on longitudinal stability of a 0.208-inch (0.007L) extension to the nose of a five-band configuration of the TX-16 are shown in figure 5. This particular configuration of the TX-16 was shown in reference 1 to have satisfactory longitudinal stability characteristics. While the level of dynamic stability at the lower Mach numbers is shown for the TX-17 to be generally the same as that of the TX-16, at the higher Mach numbers ($1.10 \leq M_0 \leq 1.20$) the modified nose appears to yield a definite trend toward higher values of $C_{m_q} + C_{m_{\dot{\alpha}}}$ for the TX-17. It is believed that some of the large differences noted in the variations of the damping derivatives with Mach number between the two configurations arise from an inherent scatter in the data which, as experience has shown, tends to increase as the moments of inertia become larger. While schlieren photographs of the TX-17 were not obtained during the investigation, the Mach number range over which the model was probably affected by the bow-wave reflection was shown by dynamic records to be between $1.10 \leq M_0 \leq 1.175$, the only range over which the model attempted to trim at other than 0° . The effect of the nose extension on the static stability parameter C_{m_α} was to produce a trend toward a slightly lower level of stability, especially in the range $0.85 \leq M_0 \leq 1.00$, where the maximum reduction in C_{m_α} of about 0.004 was noted. While a nose extension should prove beneficial to the longitudinal-stability performance from the standpoint of an improvement in the model fineness ratio, such an extension would also have a destabilizing effect on the model through an effective rearward shift in the center of gravity. At Mach numbers approaching 1.00, pressures over the model nose would constitute a particularly important factor in the stability characteristics in the model due to the reduced fin effectiveness brought about by the flow conditions noted over the afterbody in reference 1.

Short Seven.- The dynamic and static stability characteristics of the Short Seven are presented in figure 6. Because of the very low level of static stability exhibited by this model, the dynamic performance could not be recorded above $M_0 \approx 0.94$. It is noted in the figure that in addition to the problem of static stability, the Short Seven also experienced relatively low dynamic stability. Dynamic records for the Short Seven were characterized at most Mach numbers by relatively large free-model oscillations, $\pm 5^\circ$ or more. At $M_0 \approx 0.95$, the model became statically unstable or attempted to trim outside of the limits of the dynamic rig ($\pm 9^\circ$). It was ascertained by increasing the angle of attack of the support

tube that this angle of trim exceeded $+10.5^\circ$. The trim angle was reduced at $M_0 \approx 1.12$ to about $+5^\circ$ and increased with Mach number to an angle greater than $+9.5^\circ$ at $M_0 \approx 1.16$.

It is believed that the addition of the drag plate to the Short Seven, while beneficial to model damping qualities through an increased drag level of the configuration, also constituted a major destabilizing influence with respect to the flow in the vicinity of the fins. The formation of a high pressure region over the fins would tend to further reduce the effectiveness of the fins through the associated reduction in dynamic pressure.

In an effort to reduce the destabilizing pressure peaks over the forward part of the body, a single band was added to the nose of the five-band configuration of the Short Seven 1.25 inches rearward of the nose flat. While a slight increase in static stability was noted at the lower Mach numbers with the additional band, the model again was statically unstable at Mach numbers above 0.94. No additional data were obtained on this configuration.

Typical schlieren photographs of the Short Seven (fig. 6(b)) show the development and movement of the body shock patterns with changes in Mach number. It is noted from these photographs that the highly complex nature of the flow over these bodies would make attempts at correlation between changes in the body flow fields with variations in stability extremely difficult.

TX-21.- In general, changes in the model configurations did not appreciably alter the trends of the curves of dynamic and static stability with Mach number for the TX-21. Dynamic stability was shown to improve with Mach number up to Mach numbers from 0.80 to 0.85. Between Mach numbers 0.85 and 0.90, there was a rapid reduction in stability, followed by an increase in the damping rate between 0.90 and 1.00 with a leveling off tendency at higher Mach numbers. The static stability parameter $C_{m\alpha}$ was shown to have increased with Mach number up to about 0.92. A destabilizing break occurred between Mach numbers of 0.92 and 1.00 with some improvement and leveling off noted at Mach numbers above 1.00.

Schlieren photographs of a TX-21 configuration are presented for several Mach numbers in figure 7. Except for minor changes in the body flow fields due to modifications to the fins and spoiler arrangements, the flow patterns depicted in figure 7 are typical of those observed in the TX-21 investigation. The formation of compression waves was noted on the nose section at $M_0 \approx 0.75$. At subsonic speeds, this system of

shock waves, originating from the forward portion of the nose and from spoiler bands, terminated in a normal shock which moved rearward with increasing Mach number, reaching the fin leading edge at $M_0 \approx 0.94$. A high degree of turbulence or separated flow over the afterbody accompanied the appearance and movement of these discontinuities. Calculations from force data have shown that movement of the center of pressure agreed with the formation and movement of these body shocks. A rearward shift in the center of pressure noted between $0.80 \leq M_0 \leq 0.92$ was followed by a sudden forward movement in the range $0.92 \leq M_0 \leq 1.00$. Above $M_0 \approx 1.00$, the center of pressure remained generally stationary at a point slightly aft of that shown for the subsonic condition.

At a Mach number of about 1.14, schlieren photographs showed that the model was struck by the wall-reflected model bow wave (fig. 7, $M_0 = 1.203$). The strength of this asymmetrical wave reflection was not readily apparent in the schlieren system until the model length had been traversed and the disturbance intersected at the model base at $M_0 \approx 1.14$. However, dynamic records showed that for some configurations of the TX-21, the model attempted to trim in the range $1.08 \leq M_0 \leq 1.135$ with the largest trim angle occurring at the higher Mach numbers. For the majority of the TX-21 configurations, a slight increase in the amplitude of free-model oscillations only was noted at $M_0 \approx 1.135$. The effects of this disturbance may have been felt over the model base at somewhat higher Mach numbers due to the possibility of an upstream propagation of compression waves through the highly turbulent model wake.

The effects of a change in TX-21 nose contour.- The effects of modifying the contour of the TX-21 nose are shown for two test configurations in figures 8 and 9. As seen in figure 8, use of the hemispherical flat nose, nose A, on the double-wedge finned configuration improved the dynamic stability over that shown for nose B throughout the Mach number range without altering the variation of the stability coefficient $C_{m_q} + C_{m_{\dot{\alpha}}}$ with Mach number. However, this increase in dynamic stability was accompanied by a small reduction in the parameter $C_{m_{\alpha}}$ at Mach numbers above 0.85. These same effects of a change in nose contour were noted for the identical TX-21 configuration with a more forward center-of-gravity location. The effects of a change in nose shape on a configuration utilizing the $10^\circ-0^\circ$ fins are shown in figure 9. It is seen that, although these data agree with the previous effects of nose contour, there is some indication that nose A was detrimental to the dynamic stability and beneficial to static stability at Mach numbers below 0.700 and above 1.2.

Effects of a change in fin configuration on the TX-21.- Several configurations of the TX-21 were tested to evaluate the relative effectiveness of the $6^\circ-14^\circ$ double-wedge and the $10^\circ-0^\circ$ fins on longitudinal

stability. These configurations consisted of a banded and an unbanded model with nose A and a banded model with nose B. The results of this investigation are presented in figures 10 to 12.

The stability performance of the unbanded model utilizing nose A was not readily defined at all test Mach numbers due to extensive Mach number regions of dynamic and static instability. Figure 10 shows, however, that a change in fin configuration produced no discernible effects on either the magnitude or variation of $C_{m_q} + C_{m_{\dot{\alpha}}}$; possible effects at the lower Mach numbers, $0.60 \leq M_0 \leq 0.80$, are masked by the scatter in the data. A definite improvement (about 0.005) in the longitudinal static-stability parameter $C_{m_{\alpha}}$ was noted at Mach numbers below 0.85 for the 6° - 14° configuration. A more complete set of data was obtained on the banded configuration of figure 11, which is in general agreement with those of the clean model. Although these data show no significant effect on dynamic stability at subsonic Mach numbers, there is an indication that in the range $1.05 \leq M_0 \leq 1.19$, the 10° - 0° fins afforded an improvement in the level of $C_{m_q} + C_{m_{\dot{\alpha}}}$. However, use of the 6° - 14° fins produced a definite increase in the magnitude of the longitudinal static-stability coefficient $C_{m_{\alpha}}$ at all test Mach numbers except 0.70 and 1.20. Tests of nose B on a banded configuration of the TX-21 (fig. 12) showed that the 10° - 0° fins gave marked improvement to the dynamic-stability performance particularly in the range $0.90 \leq M_0 \leq 1.00$ where the configuration with 6° - 14° fins showed a rapidly destabilizing trend. The static-stability characteristics of this configuration agreed with the data from the banded nose A configuration, in that the double-wedge fins produced an increase in $C_{m_{\alpha}}$ of about 0.005 at all test Mach numbers below 1.00.

Effects of spoiler bands on the TX-21.- To evaluate the effects of spoiler bands on the longitudinal stability of the TX-21, tests were conducted by varying both the number and arrangement of the bands for several nose and fin configurations (figs. 13 and 14).

As seen in figure 13, for which nose A and the 10° - 0° fins were utilized, the major effect on dynamic stability accompanied the addition of bands 2 and 3 to the clean model. An examination of high-speed schlieren motion pictures in reference 2 indicated that, for bodies of a type similar to those of the present investigation, the effect of the spoiler-band addition was to stabilize a large fore-and-aft movement of the body shocks as the model oscillated. The close control of the body flow field maintained by the spoiler bands is emphasized by the data of figure 13 in that the use of two additional bands on the afterbody did not alter the dynamic-stability characteristics significantly. However, as seen in table II, configurations 11, 12, and 13, the model

was highly sensitive to flow changes over the nose section by the addition of band 1.

The addition of bands to the clean model also improved the static-stability performance of this configuration of the TX-21, especially at Mach numbers above 0.93 where instability was noted for the clean configuration. Changing from a two to a three band configuration also improved the level of $C_{m\alpha}$ at Mach numbers above 1.00. This is in agreement with the data of reference 1 wherein it was shown that increasing the size or number of bands on the TX-16 yielded substantial improvements in static stability. These same effects of spoiler-band addition were noted for a 6° - 14° double-wedge finned configuration of the TX-21 with nose A. (fig. 14).

Several configurations of the TX-21 were also tested utilizing nose B in conjunction with the 6° - 14° fins (fig. 15). It is seen from these data that rearranging the bands as shown produced a displacement of the curve of $C_{mq} + C_{m\dot{\alpha}}$ to a lower Mach number region ($\Delta M_0 \approx 0.015$) without changing the character of the results. The data also show that some improvement in static stability may be realized by a judicious arrangement of the spoiler bands on the body.

The effects of center of gravity on the TX-21.- The results of several investigations of the effect of movement in the center of gravity on the longitudinal stability of the TX-21 are presented in figures 16 and 17. In figure 16, it is seen that a forward movement in center of gravity of 0.076L for the TX-21 with nose A improved the level of dynamic stability for all test Mach numbers. Tests of the TX-21 with nose B and with a shift in the center of gravity by a like amount (0.076L), figure 17, was in agreement with this increase. Changes in static stability with center-of-gravity position agreed with calculations from force data with the higher levels of $C_{m\alpha}$ shown for the more forward center-of-gravity position.

Reynolds number effects on TX-21.- In previous investigations in the 8-foot transonic pressure tunnel of bodies similar in size and external shape to the models of this investigation (refs. 1 and 2), attempts were made to determine the effects of Reynolds number on the longitudinal dynamic and static-stability coefficients. However, results of these investigations showed no conclusive trends within the Reynolds number range of the tests. In an effort to define Reynolds number effects on the TX-21, several configurations were tested at stagnation-pressure levels of both 1.0 and 0.6 atmosphere (figs. 18 and 19). In addition, one configuration was tested at 0.6 atmosphere with and without the addition of artificial roughness to the nose and afterbody (fig. 20).

Changing the stagnation pressure level and increasing the Reynolds number from about 1.0 to 1.4×10^6 to about 1.5 to 2.1×10^6 (fig. 18) aggravated the trend toward dynamic instability noted at 0.6 atmosphere for $0.85 \leq M_0 \leq 0.94$ with the model becoming unstable at 1.0 atmosphere over this Mach number range. The proximity to a critical Reynolds number was evidenced during the investigation when relatively small reductions in the tunnel total pressure alleviated the divergent free-model oscillations observed over the aforementioned Mach number range. Some effect of Reynolds number is also noted on the static-stability coefficient $C_{m\alpha}$ in figure 18. Increasing the stagnation pressure improved the stability of the configuration in the Mach number range $0.80 \leq M_0 \leq 0.90$. This configuration at both Reynolds numbers (pressures) was observed to trim at a maximum angle of -5° in the Mach range $0.93 \leq M_0 \leq 0.975$.

The effects of changing stagnation pressure (Reynolds number) on the banded configuration of the TX-21 are shown in figure 19. These data emphasize the highly restrictive influence of the spoiler bands on the boundary layer in that no major effects of Reynolds number are indicated for either the dynamic- or static-stability characteristics.

In an effort to increase the effective Reynolds number of the TX-21, the clean configuration was tested, with nose A and the 6° - 14° fins, at 0.6 atmosphere with and without artificial roughness applied to the model nose and afterbody. The roughness consisted of 100-mesh carborundum grains attached to the model with a commercial plastic spray. A 0.750-inch strip was applied with the leading edge 1.188 inches rearward of the nose flat, while a 0.688-inch strip was applied to the afterbody at the 4.125-inch model station. The results of this investigation (fig. 20) show that the effects of roughness was to reduce the level of the rotational damping coefficient except at the lowest and highest test Mach numbers. This reduction was of sufficient magnitude that the model became dynamically unstable for $0.85 \leq M_0 \leq 0.96$. Large free-model oscillations ($\pm 9^\circ$) in the Mach range $0.825 \leq M_0 \leq 0.925$ were indicated for the model with roughness while such oscillations were not noted for the clean configuration.

The static-stability parameter $C_{m\alpha}$ was increased by the addition of roughness at all subsonic Mach numbers, particularly at $M_0 \approx 0.90$. Static instability, noted at $M_0 \approx 0.94$ for the clean model, was not indicated for the configuration with roughness.

It should be noted that for those conditions where the Reynolds number was varied by changing the tunnel pressure level, the model damping characteristics may have been influenced by important dynamic effects not wholly associated with Reynolds number. However, a comparison of the data in figures 18 to 20 would indicate such effects to

be of a secondary nature and that the described stability changes resulted primarily from scale effects.

CONCLUDING REMARKS

Investigations of the longitudinal stability characteristics of the TX-17, Short Seven, and TX-21 specialized store configurations have indicated the following results:

The addition of a 0.208-inch (0.007L) extension to the nose of a five-band configuration of the TX-16 to obtain the TX-17 configuration increased the level of dynamic stability at the higher Mach numbers ($1.10 \leq M_0 \leq 1.2$), while the stability level remained essentially unchanged at the lower Mach numbers. Only minor reductions in static stability resulted from use of the modified nose; the maximum reduction in $C_{m\alpha}$ was noted to be about 0.004 in the range $0.85 \leq M_0 \leq 1.00$.

The Short Seven store configuration was shown to have experienced a low level of dynamic stability as well as only marginal static stability at all test Mach numbers less than 0.95. At higher Mach numbers, the configuration was shown to be statically unstable.

An investigation of the effects of a change in nose contour on the longitudinal stability of the TX-21 showed that the hemispherical flat nose, nose A, improved the dynamic stability over most of the test Mach number range while the two-radius ogive flat nose, nose B, was beneficial from a static stability standpoint for the same Mach numbers. A change in the TX-21 fin configuration by replacement of 6° - 14° double-wedge fins with 10° - 0° fins resulted in only minor effects on dynamic stability, whereas the static-stability parameter $C_{m\alpha}$ was generally reduced by about 0.005. The addition of two spoiler bands to a clean configuration of the TX-21 produced significant improvements in both dynamic and static stability. Increasing the number of bands or judicious rearrangement of the bands generally improved the static-stability performance at Mach numbers above 1.00. A forward movement in the center of gravity of 0.076L on several TX-21 configurations was beneficial to the level of both the dynamic and static stability. An investigation of the effects of Reynolds number on the TX-21 showed that increasing the effective Reynolds number by changes in the tunnel pressure level or by the addition of artificial

roughness reduced the dynamic stability performance of the clean configuration while generally improving the level of static stability. No effects of Reynolds number were noted on configurations where the boundary layer was primarily controlled by spoiler bands.

Langley Aeronautical Laboratory,
National Advisory Committee for Aeronautics,
Langley Field, Va., December 1, 1954.

Beverly Z. Henry, Jr.
for John A. Braden
Aeronautical Research Scientist

Approved:

Eugene C. Draley
Eugene C. Draley

Chief of Full Scale Research Division

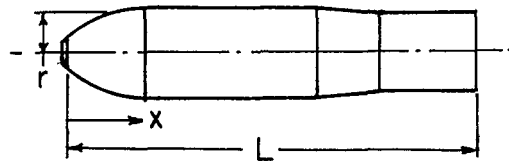
epr

REFERENCES

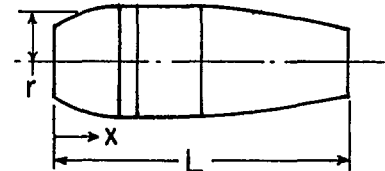
1. Braden, John A., and Henry, Beverly Z., Jr.: An Investigation of the Longitudinal Stability and Afterbody Pressure Characteristics of Specialized Store Configurations at Transonic Speeds. NACA RM SL54C24, 1954.
2. Henry, Beverly Z., Jr., and Braden, John A.: An Investigation of the Dynamic and Static Stability Characteristics of a Group of Specialized Store Configurations at Transonic Speeds. NACA RM SL53G09c, 1953.

TABLE I

BODY COORDINATES FOR THE TX-17 AND SHORT SEVEN MODELS



TX-17



Short Seven

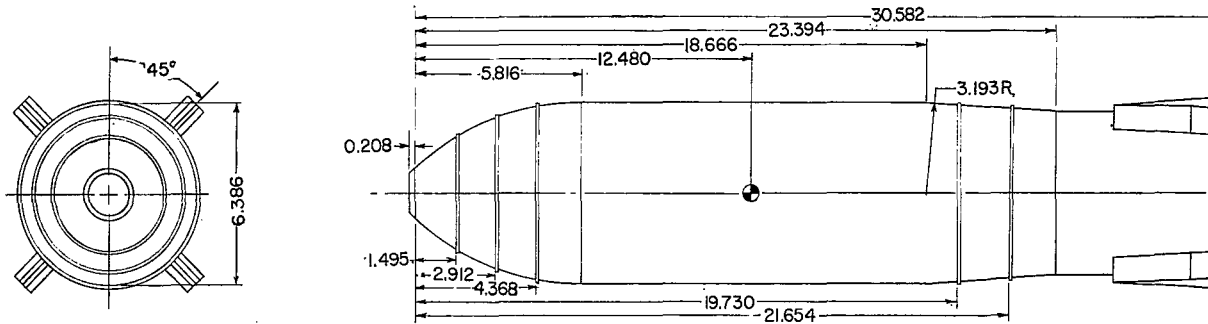
TX-17			
x, in.	r, in.	x, in.	r, in.
-0.208	0.799	3.328	2.833
.000	.988	3.536	2.891
.208	1.166	3.744	2.945
.416	1.334	3.952	2.993
.624	1.491	4.160	3.035
.832	1.639	4.368	3.073
1.040	1.779	4.576	3.105
1.248	1.910	4.784	3.132
1.456	2.033	4.992	3.154
1.664	2.148	5.200	3.171
1.872	2.256	5.408	3.183
2.080	2.358	5.616	3.191
2.288	2.452	5.816	3.193
2.496	2.540	18.666	3.193
2.704	2.622	23.394	2.873
2.912	2.698	30.582	2.873
3.120	2.768		
L = 30.790			

Short Seven			
Nose		Afterbo	
x, in.	r, in.	x, in.	
0.000	2.314	5.000	
.346	2.484	6.250	
.686	2.743	10.880	
1.029	2.913	11.380	
1.371	3.063	11.880	
1.714	3.193	12.380	
2.057	3.306	12.880	
2.400	3.404	13.380	
2.743	3.488	13.880	
3.086	3.559	14.880	
3.429	3.619	15.880	
3.771	3.667	16.630	
4.114	3.703	17.505	
4.457	3.729	17.880	
4.800	3.745	18.130	
5.000	3.750	21.880	
L = 21.880			

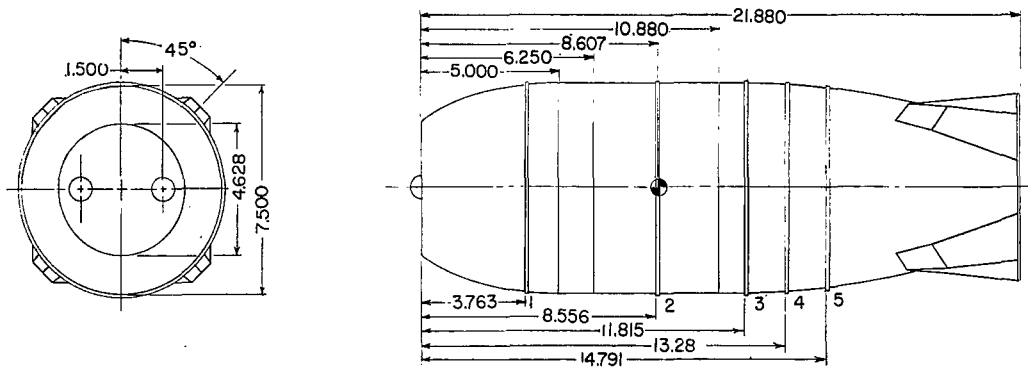
TABLE II
SUMMARY OF MAJOR TEST RESULTS



Configuration	Model	Nose	Fins	Spoiler arrangement	C.G., percent L	I, slug-ft ²	Stagnation pressure, atm	Remarks
1	TX-17	Ogive	50-50° 6°-14°	1-2-3-12-13	41.2	0.5071	1.00	Dynamic stability improved over TX-16 for 1.10 ≤ M ₀ ≤ 1.2; reduction in static stability for 0.85 ≤ M ₀ ≤ 1.0.
2	Short Seven	Elliptical	5°-25°	2-3-4-5	39.3	0.3779		Low dynamic and static stability; statically unstable above M ₀ ≈ 0.94.
3				1-2-3-4-5	↓		↓	No improvement over configuration 2.
4	TX-21	Hemispherical flat	6°-14°	None	40.3	0.1552	0.60	Roughness on nose and afterbody.
5							↓	Dynamic stability improved over configuration 4; static stability reduced.
6							1.00	Dynamic stability reduced with increase in pressure for 0.85 ≤ M ₀ ≤ 0.95; static stability increased over configuration 5.
7				2-3-5-7		0.1541		Extensive improvements in dynamic and static stability over configuration 6.
8				2-4-6-8				Improvement in dynamic stability for M ₀ > 1.00; some reduction in static stability.
9					32.7	0.1878		Improvements in dynamic and static stability.
10			10°-0°	None	40.3			Dynamically unstable for M ₀ > 0.85; statically unstable for M ₀ > 0.95.
11				2-3		0.1551		Model dynamically and statically stable.
12				1-2-3				Neutrally stable up to M ₀ ≈ 0.875; dynamically unstable at M ₀ > 0.875.
13				1-3				No improvement over configuration 12.
14				2-3-5				Dynamic stability about same as configuration 11; improvement in C _{mα} noted for M ₀ ≥ 1.00.
15				2-3-5-7				Stability characteristics about same as configuration 14.
16		Two-radius ogive flat	6°-14°	2-4-6-8	32.8	0.1889	0.60	Dynamically and statically stable at all Mach numbers.
17							1.00	Stability characteristics about the same as configuration 16.
18					40.4	0.1607		Dynamic and static stability improved over configuration 17.
19				2-3-5-7		0.1614		Improvement in static stability over configuration 18.
20			10°-0°			0.1603		Improvement in dynamic stability over configuration 19. Static stability level reduced.



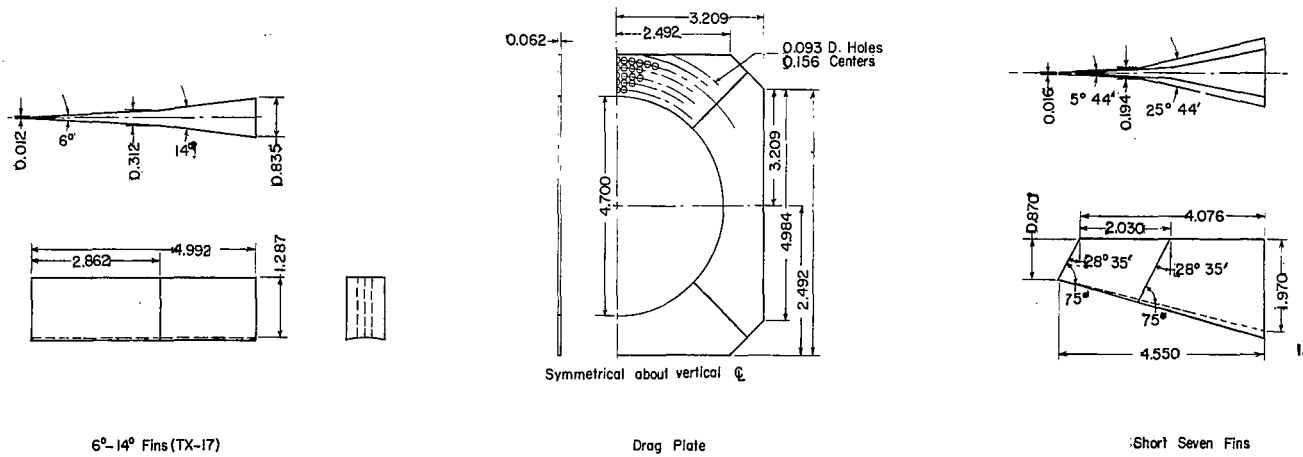
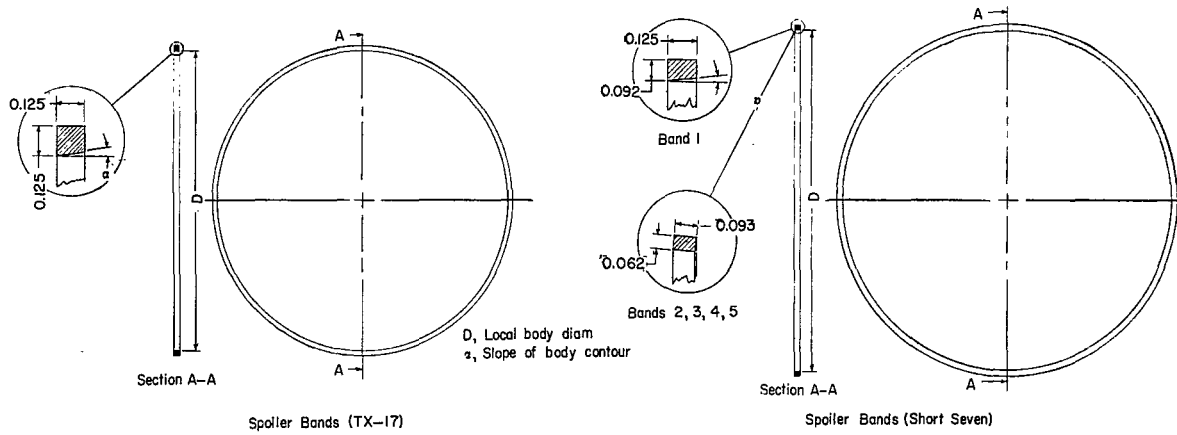
TX-17



SHORT SEVEN

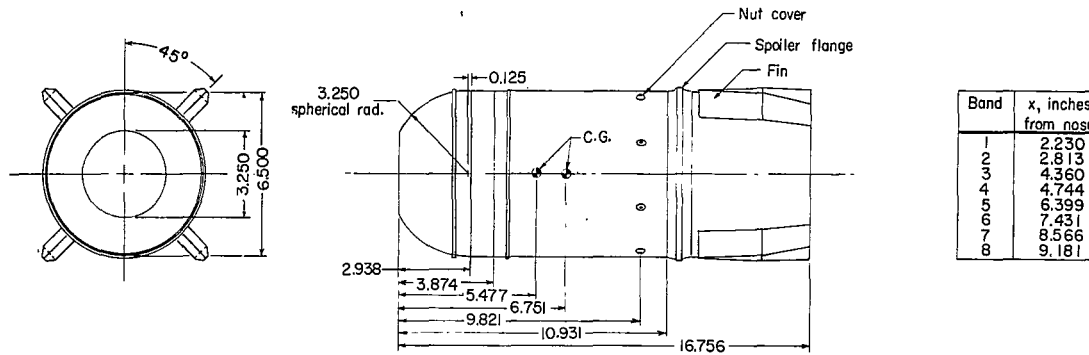
(a) Model details.

Figure 1.- Details of the TX-17 and "Short Seven" test configurations.
All dimensions are in inches.

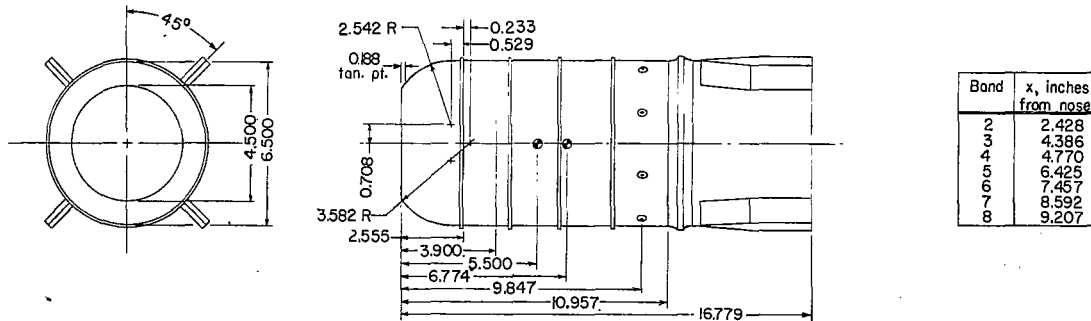


(b) Details of the TX-17 and "Short Seven" accessory parts.

Figure 1.- Concluded.



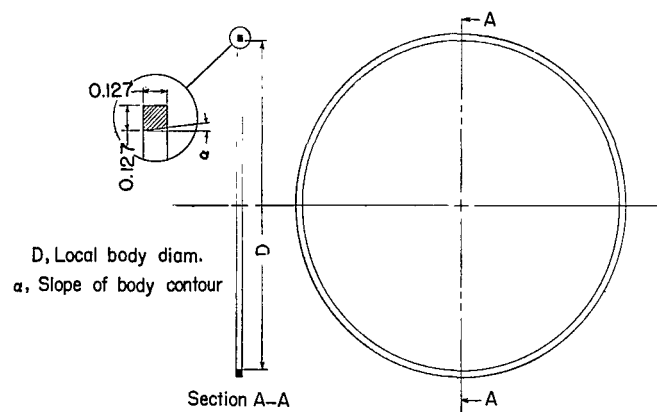
Hemispherical-Flat Nose Configuration (Nose A)



Two-Radius Ogive-Flat Nose Configuration (Nose B)

(a) Model details.

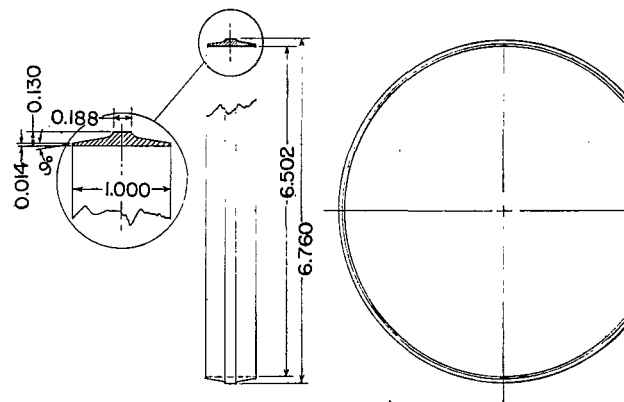
Figure 2.- Details of the TX-21 test configurations. All dimensions are in inches.



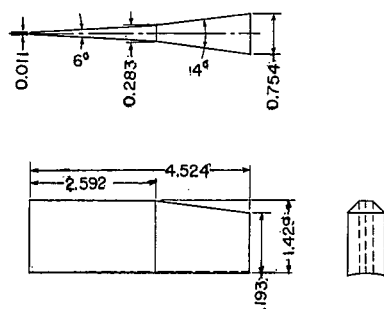
D, Local body diam.
 α , Slope of body contour

Section A-A

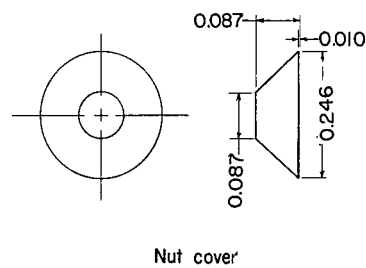
Spoiler Band



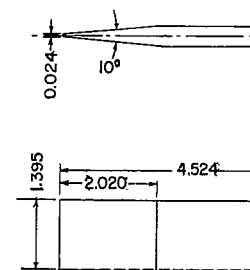
Spoiler Flange



6°-14° Fins (TX-21)



Nut cover



10° Fins (TX-21)

(b) Details of the TX-21 accessory parts.

Figure 2.- Concluded.

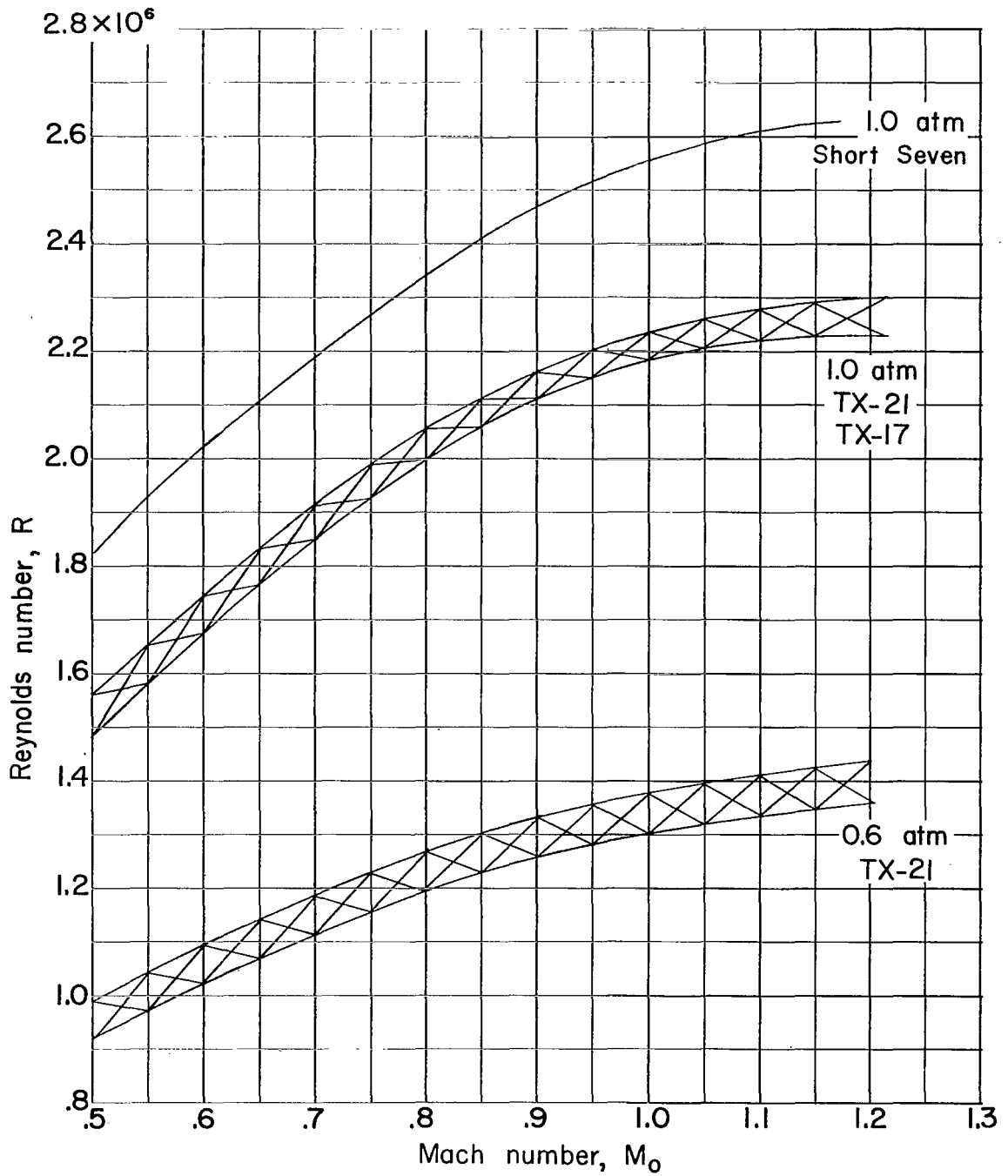
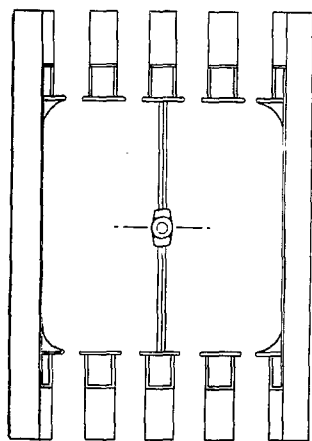


Figure 3.- Variation of Reynolds number in the Langley 8-foot transonic pressure tunnel.



Section A-A

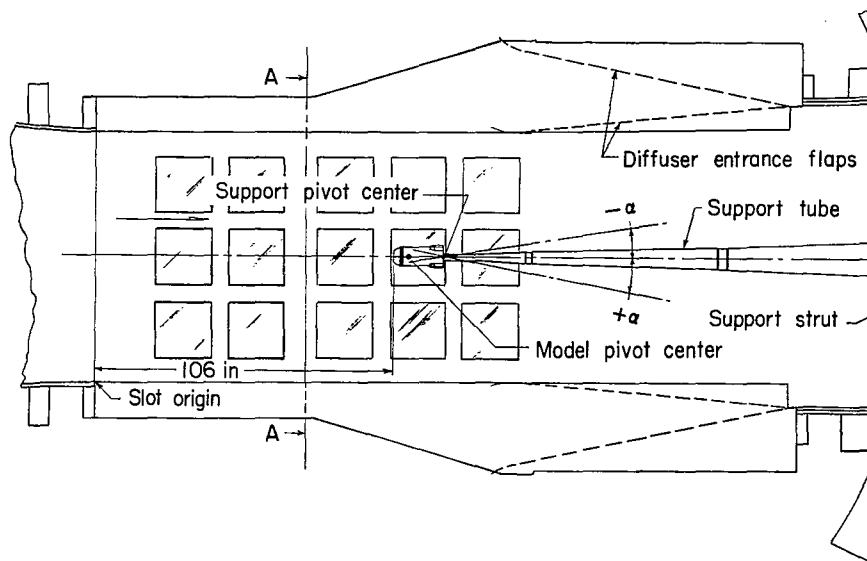


Figure 4.- General arrangement of a typical model installation in the Langley 8-foot transonic pressure tunnel. All dimensions are in inches.

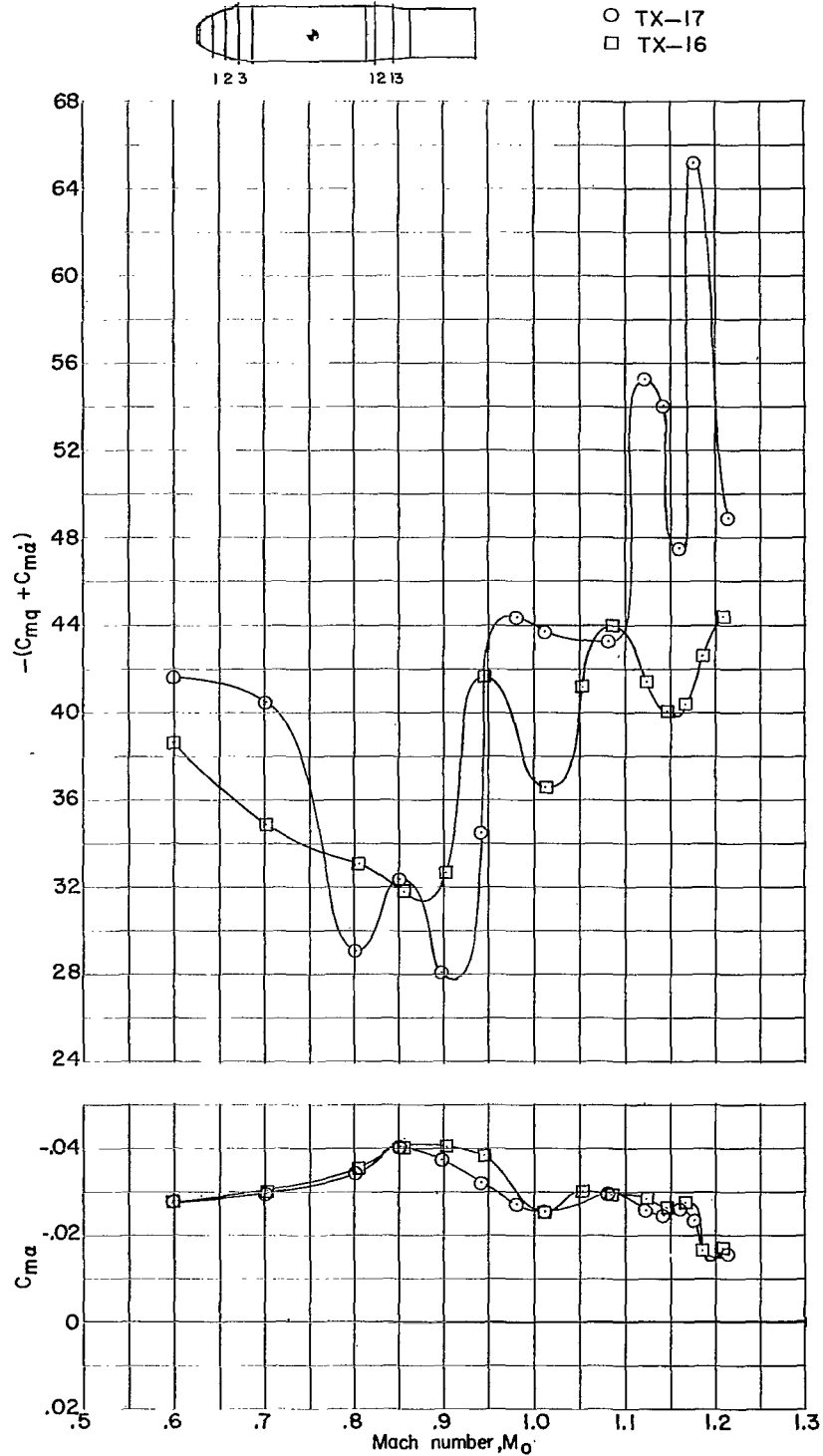
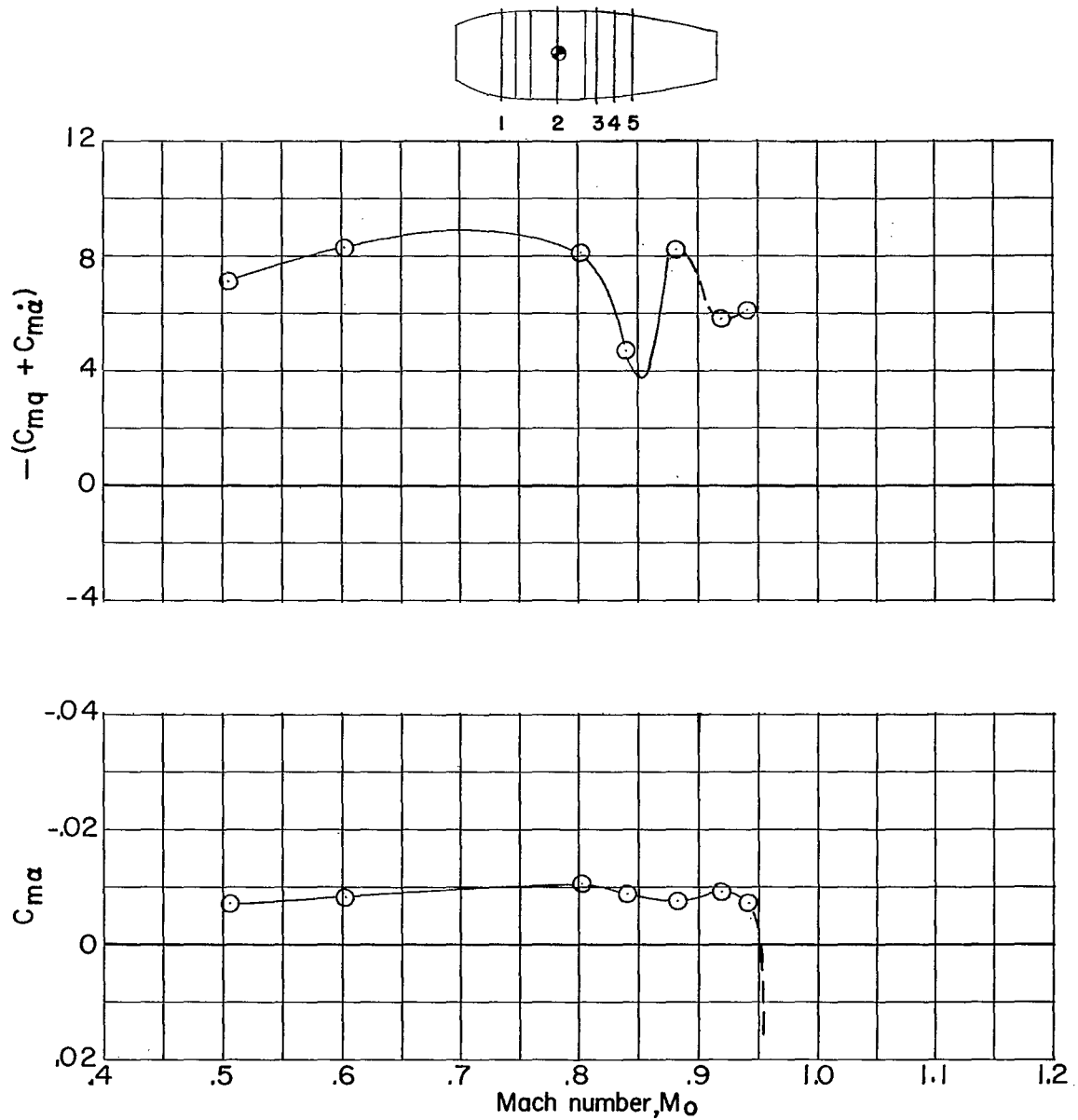
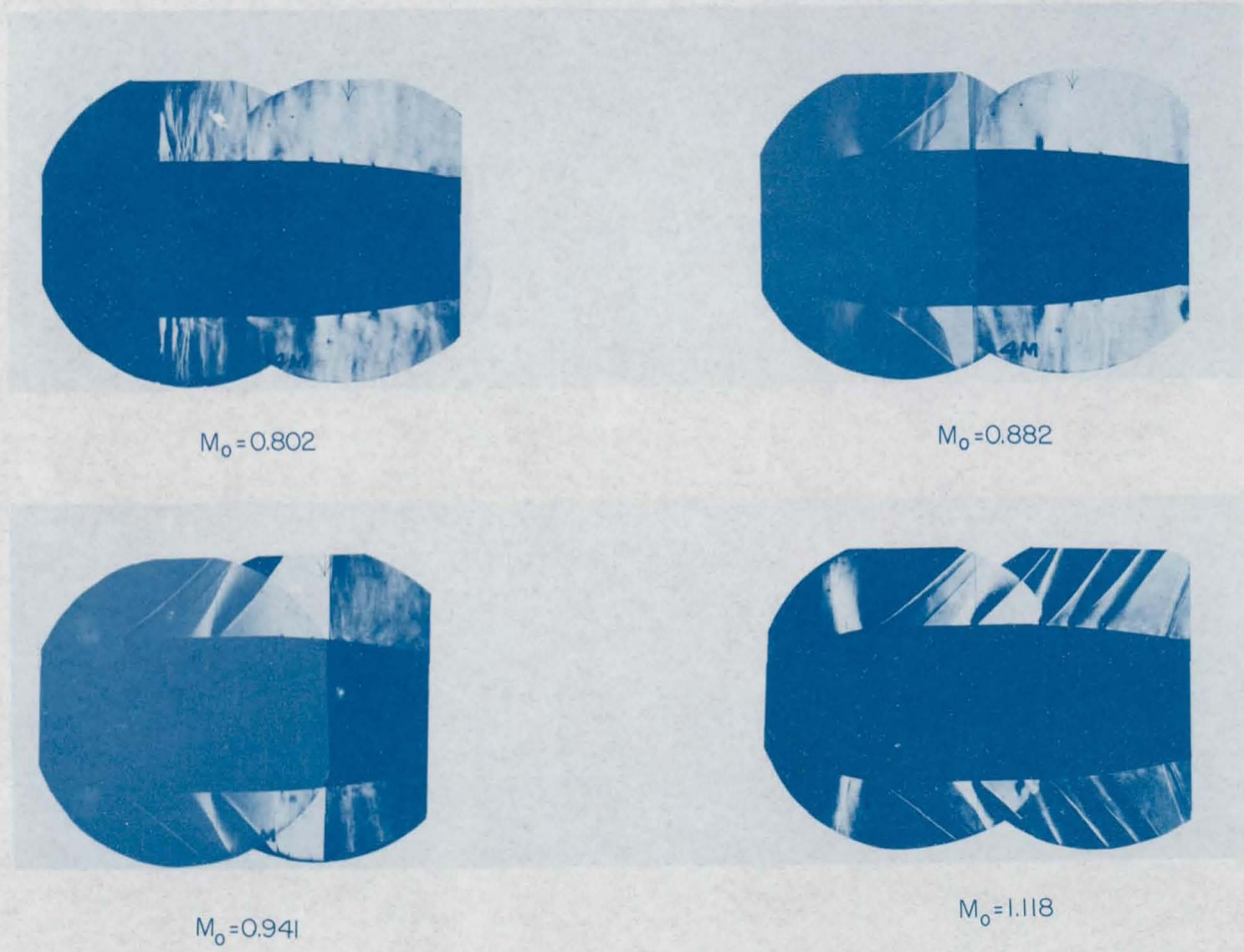


Figure 5.- The effects of a 0.208-inch nose extension (TX-17) on the longitudinal stability of the TX-16.



(a) Dynamic and static stability.

Figure 6.- The longitudinal stability performance of the "Short Seven" configuration.



(b) Schlieren photographs of the "Short Seven."

L-87527

Figure 6.- Concluded.

SECRET

SECRET

SECRET

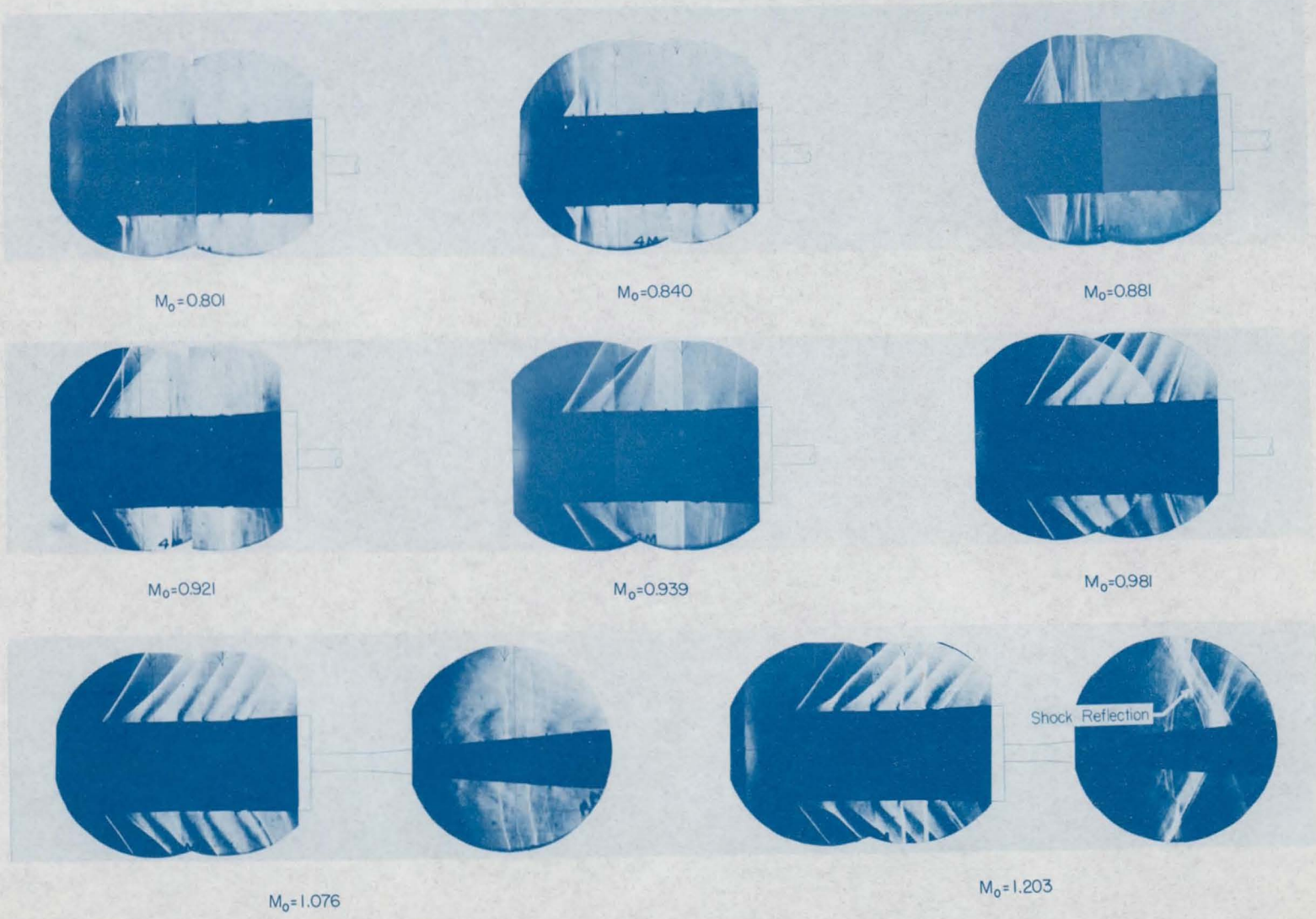


Figure 7.- Schlieren photographs of a typical TX-21 test configuration. L-87528

Full scale
Drop tests
+ Reeves Gyro
⊕ Summers Gyro

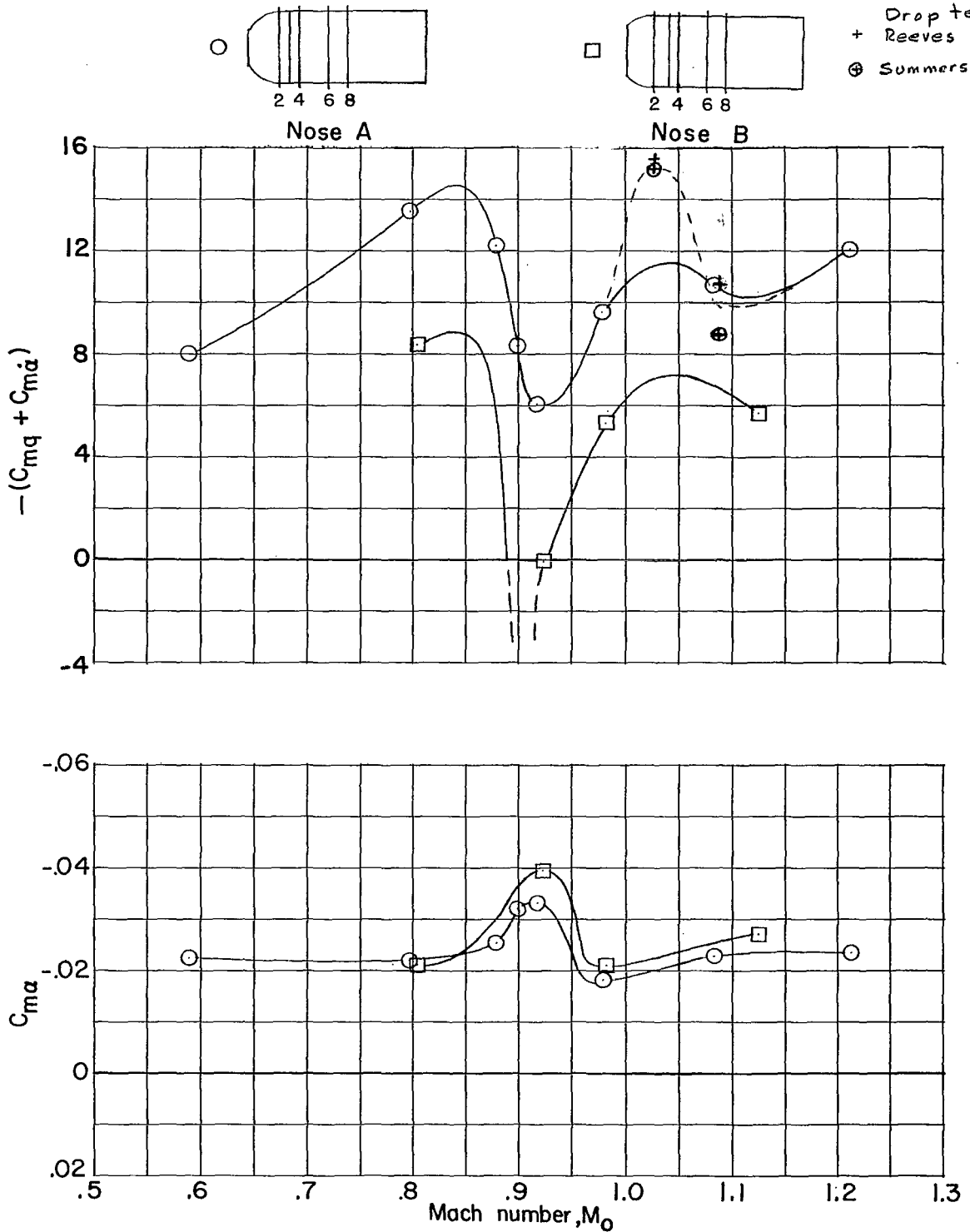


Figure 8.- The effect on longitudinal stability of a modification to the TX-21 nose contour utilizing the 6° - 14° double-wedge fins.

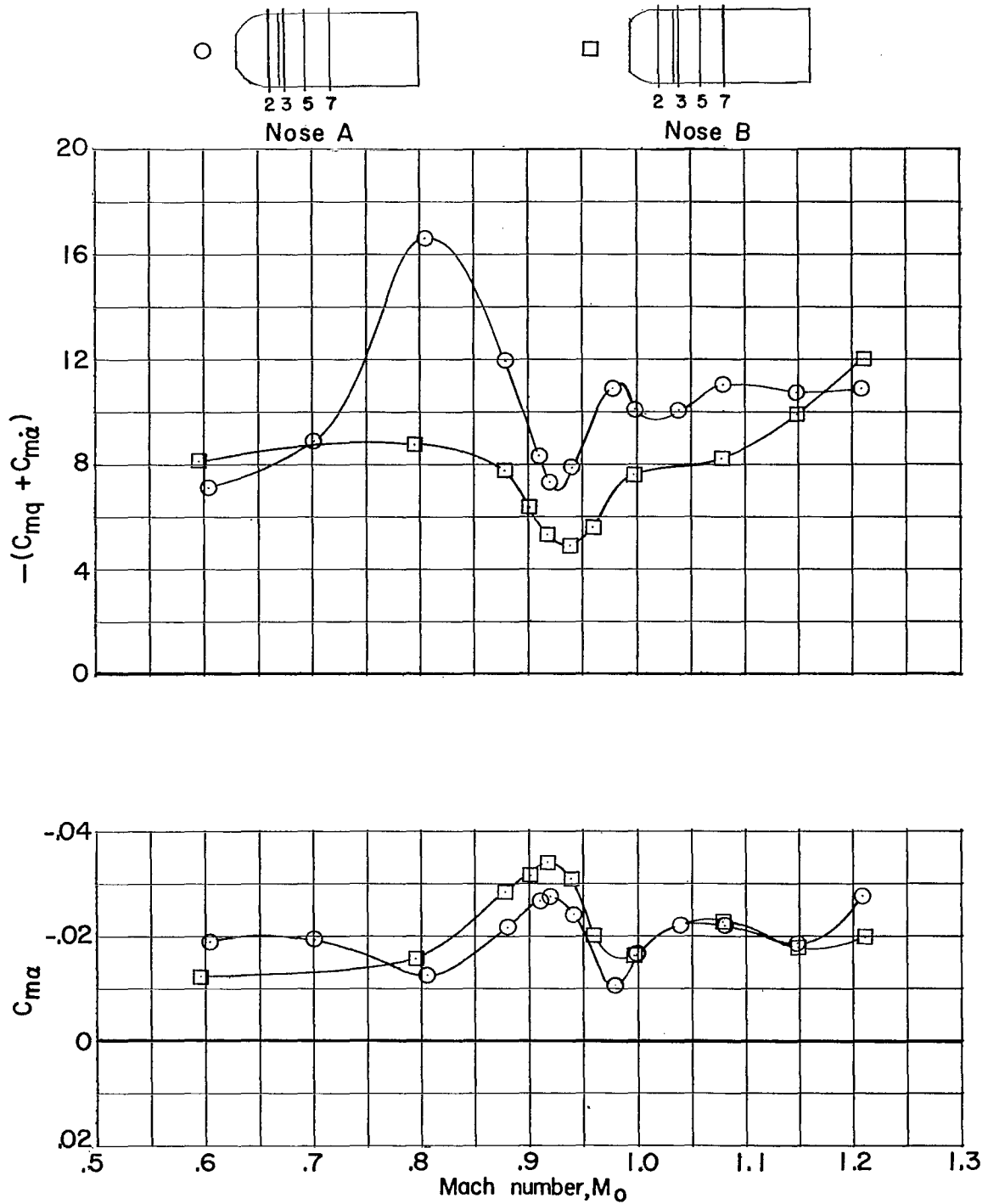


Figure 9.- The effects on longitudinal stability of a modification to the TX-21 nose contour utilizing the $10^{\circ}-0^{\circ}$ fins.



○ 6°-14° Fins ✓ OK at Full scale
 □ 10°-0° Fins

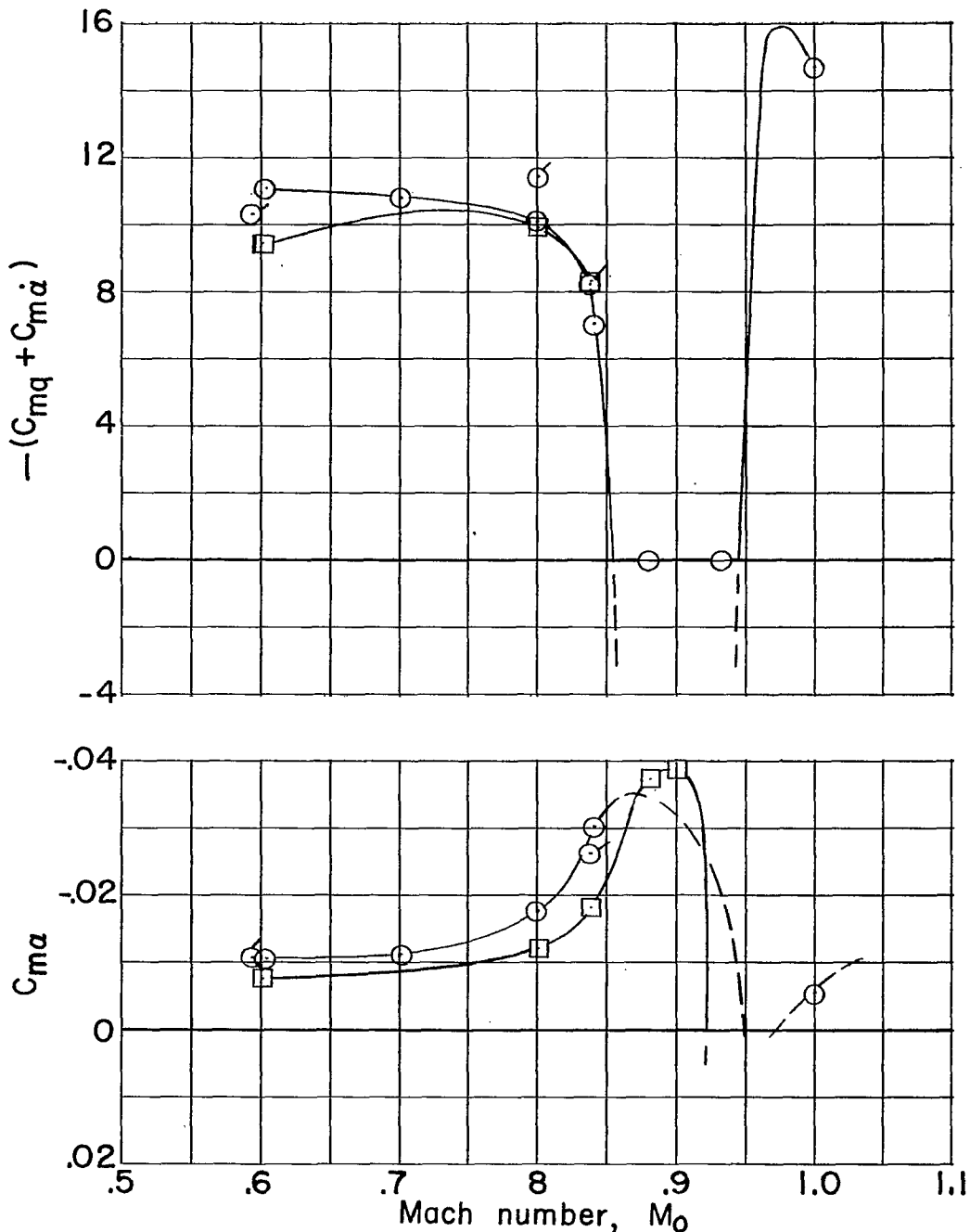


Figure 10.- The effects of a fin change on the longitudinal-stability performance of a clean configuration of the TX-21 utilizing nose A.

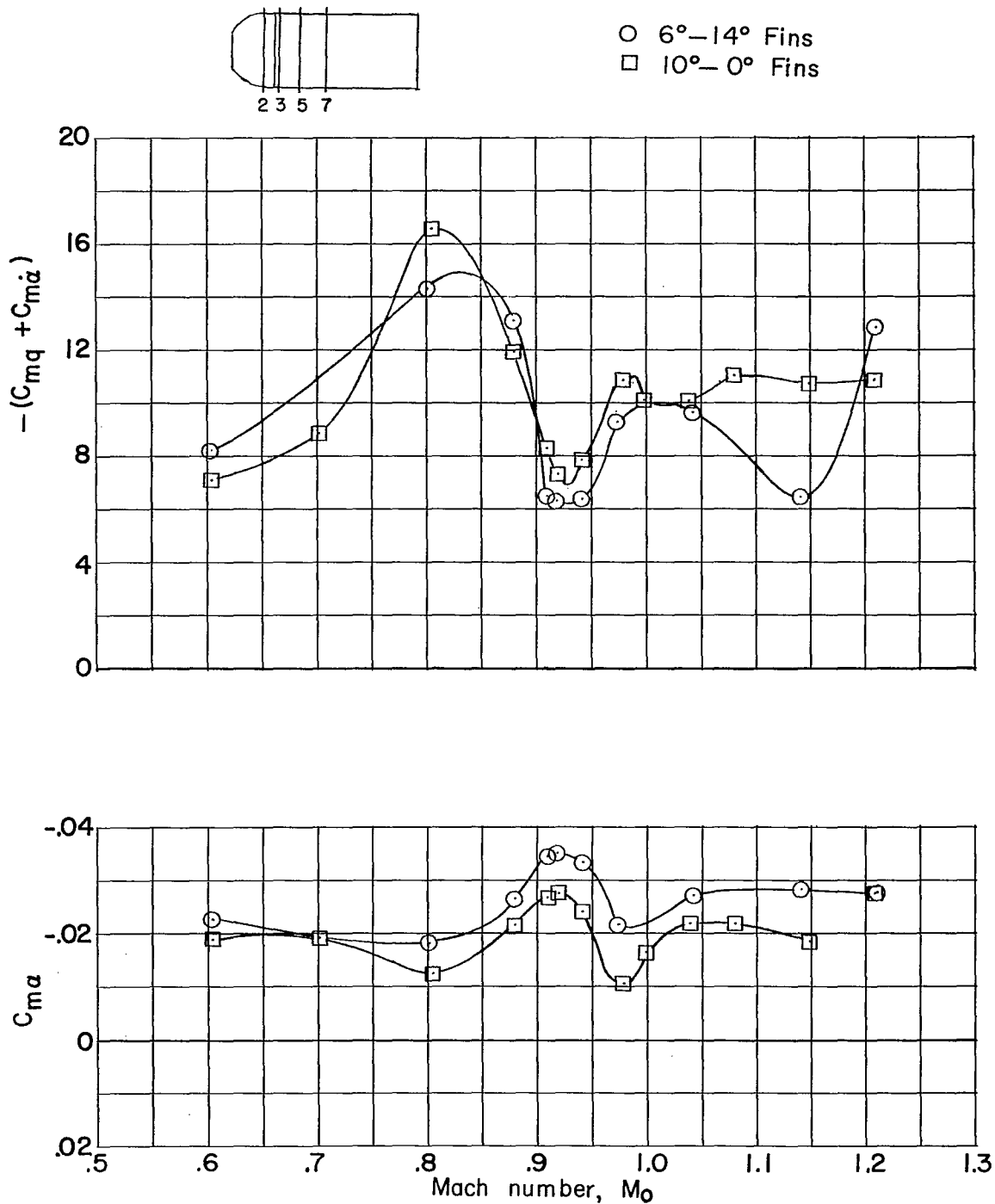


Figure 11.- The effects of a fin change on the longitudinal-stability performance of a banded configuration of the TX-21 utilizing nose A.

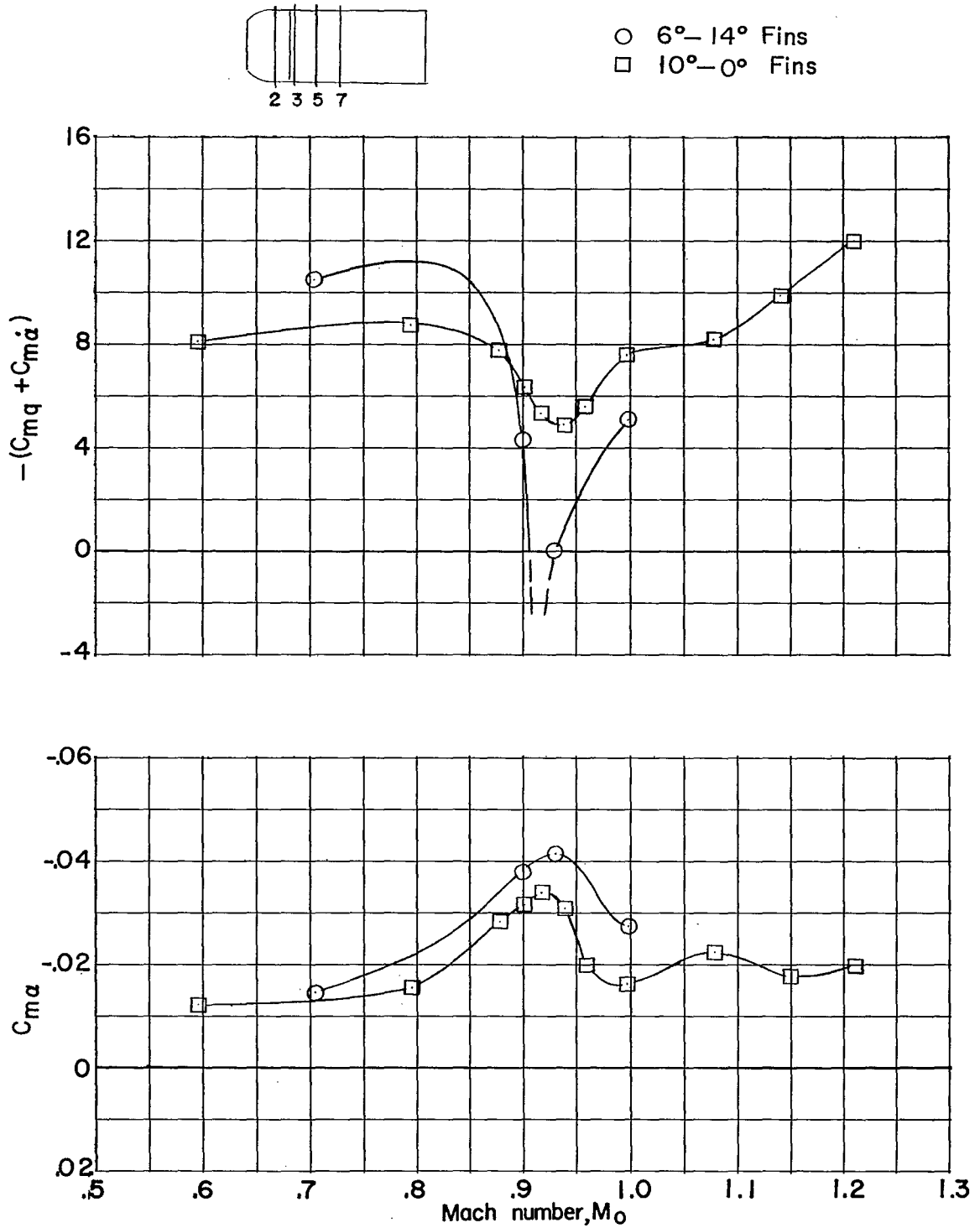


Figure 12.- The effects of a fin change on the longitudinal-stability performance of a banded configuration of the TX-21 utilizing nose B.

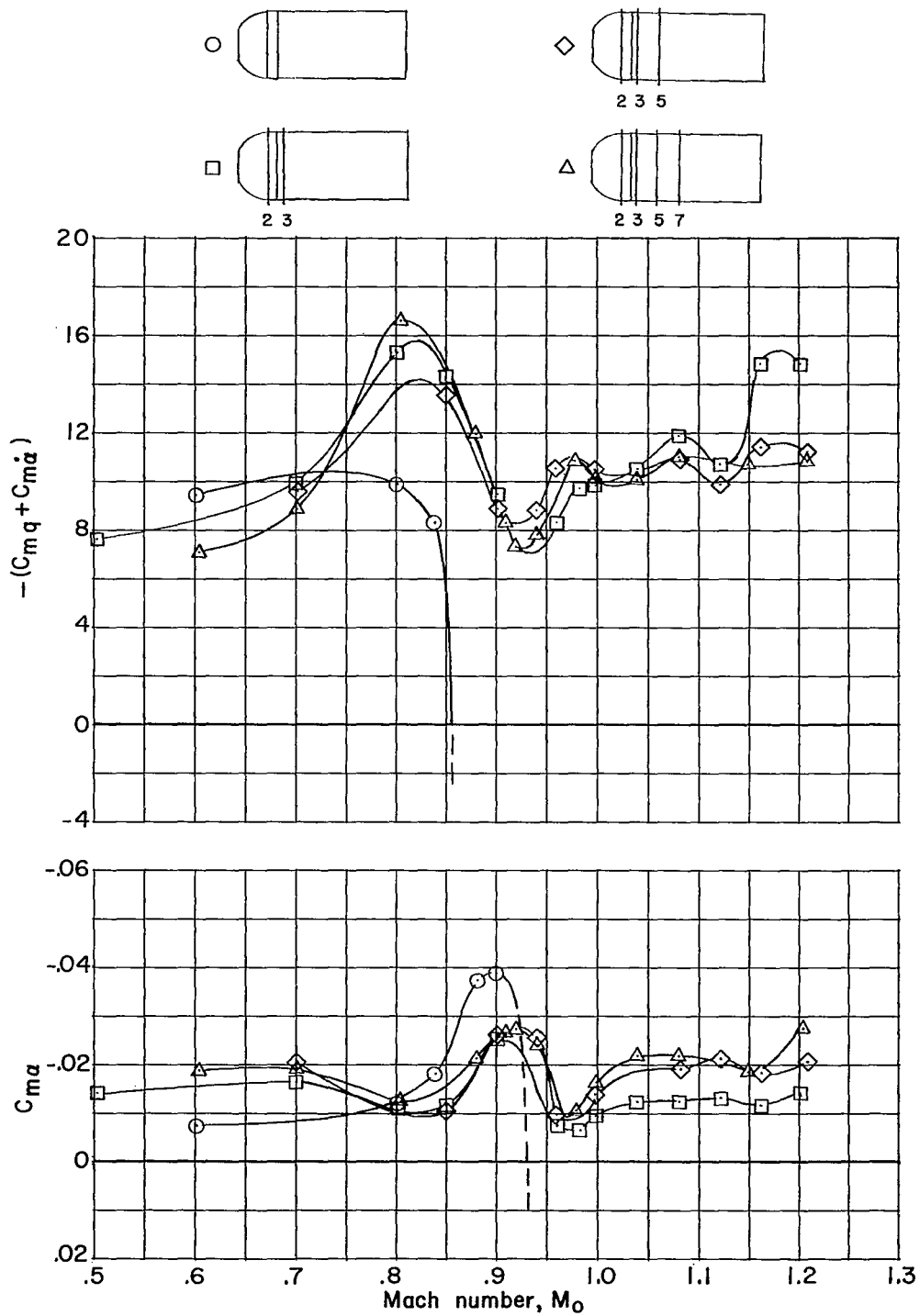


Figure 13.- The effects of spoiler-band addition and arrangement on the longitudinal stability characteristics of a TX-21 configuration with nose A and the 10^0-0^0 fins.

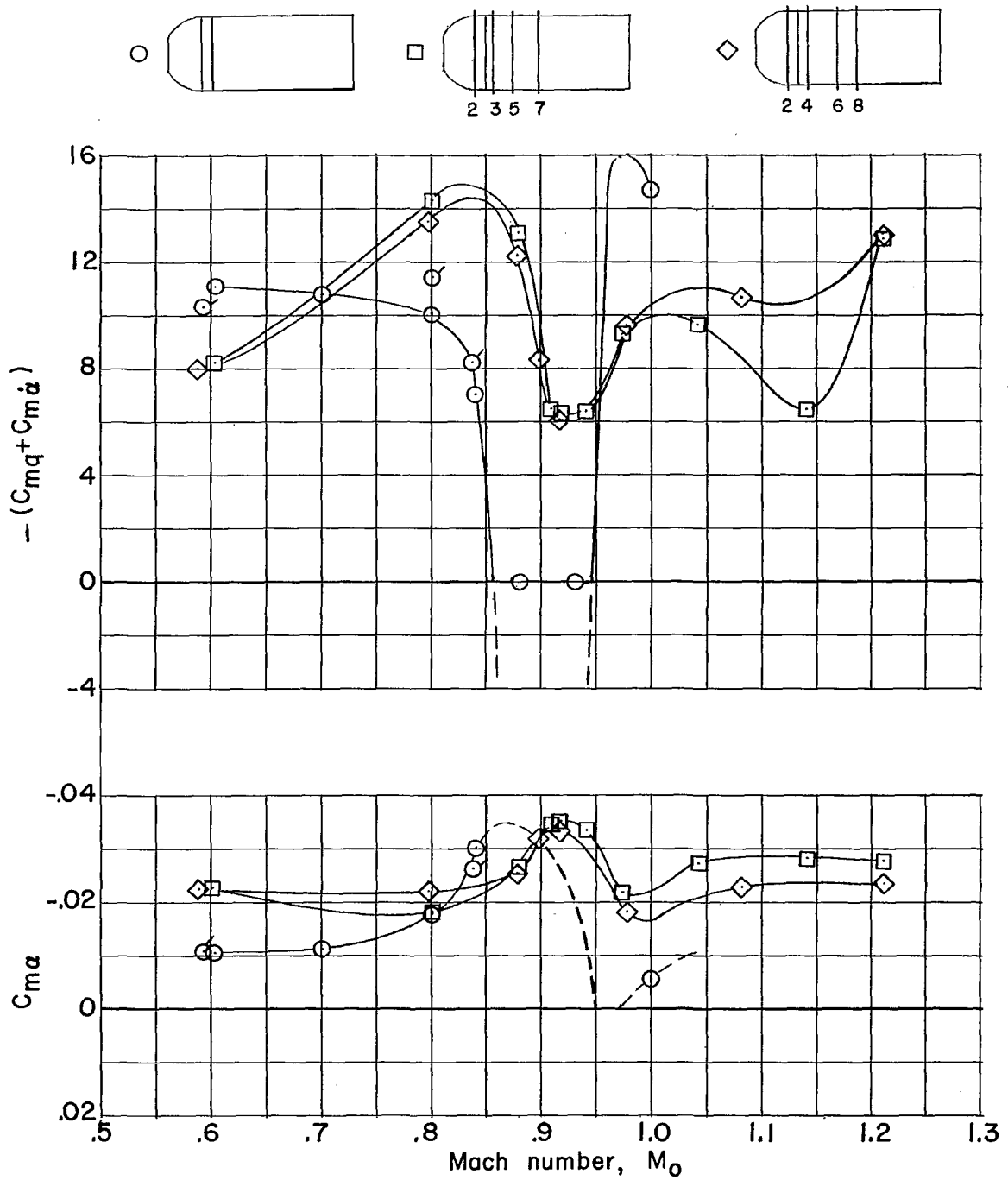


Figure 14.- The effects of spoiler-band addition and arrangement on the longitudinal stability characteristics of a TX-21 configuration with nose A and the 6° - 14° fins.

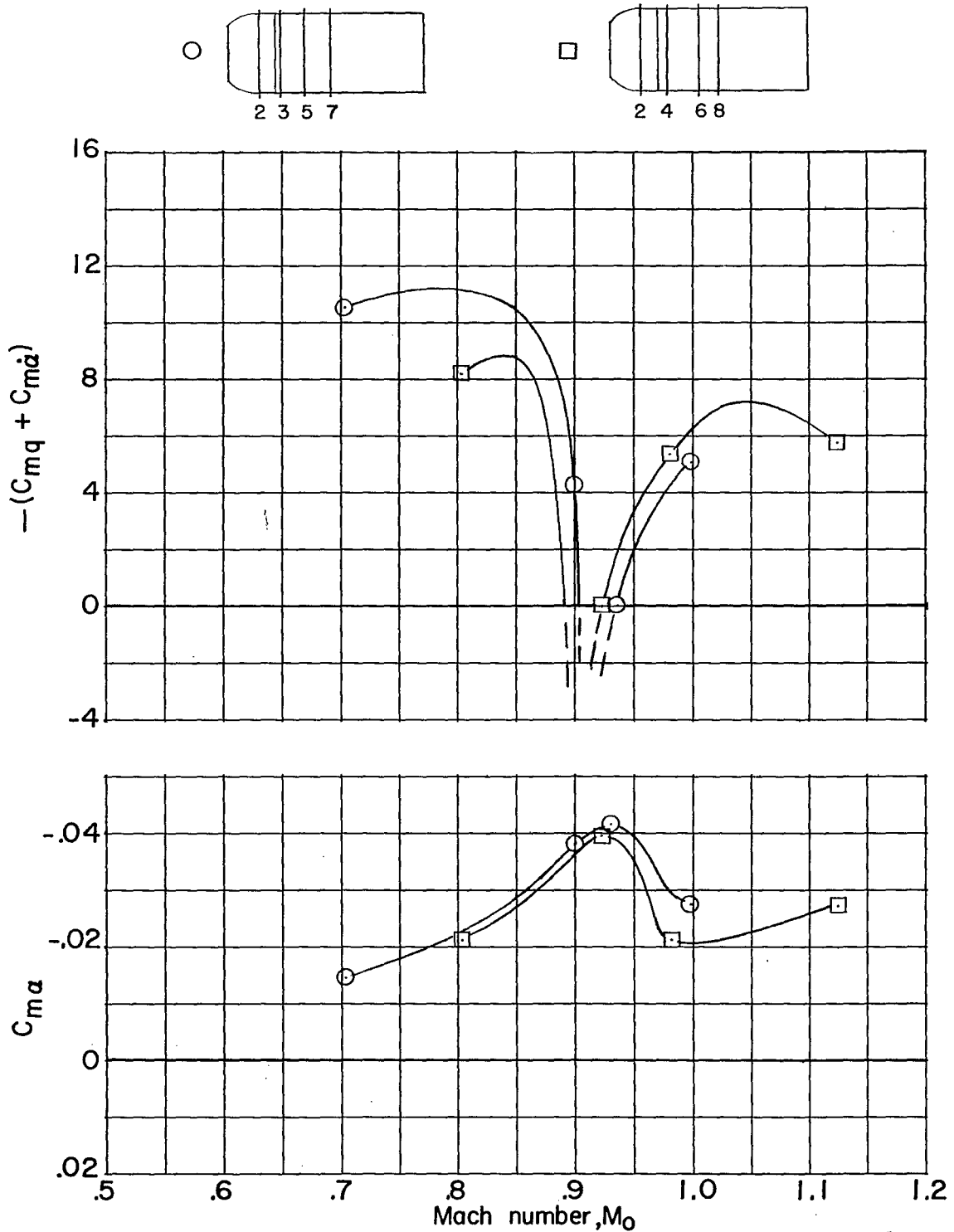


Figure 15.- The effects of spoiler-band arrangement on a TX-21 configuration utilizing nose B and the 6°-14° fins.

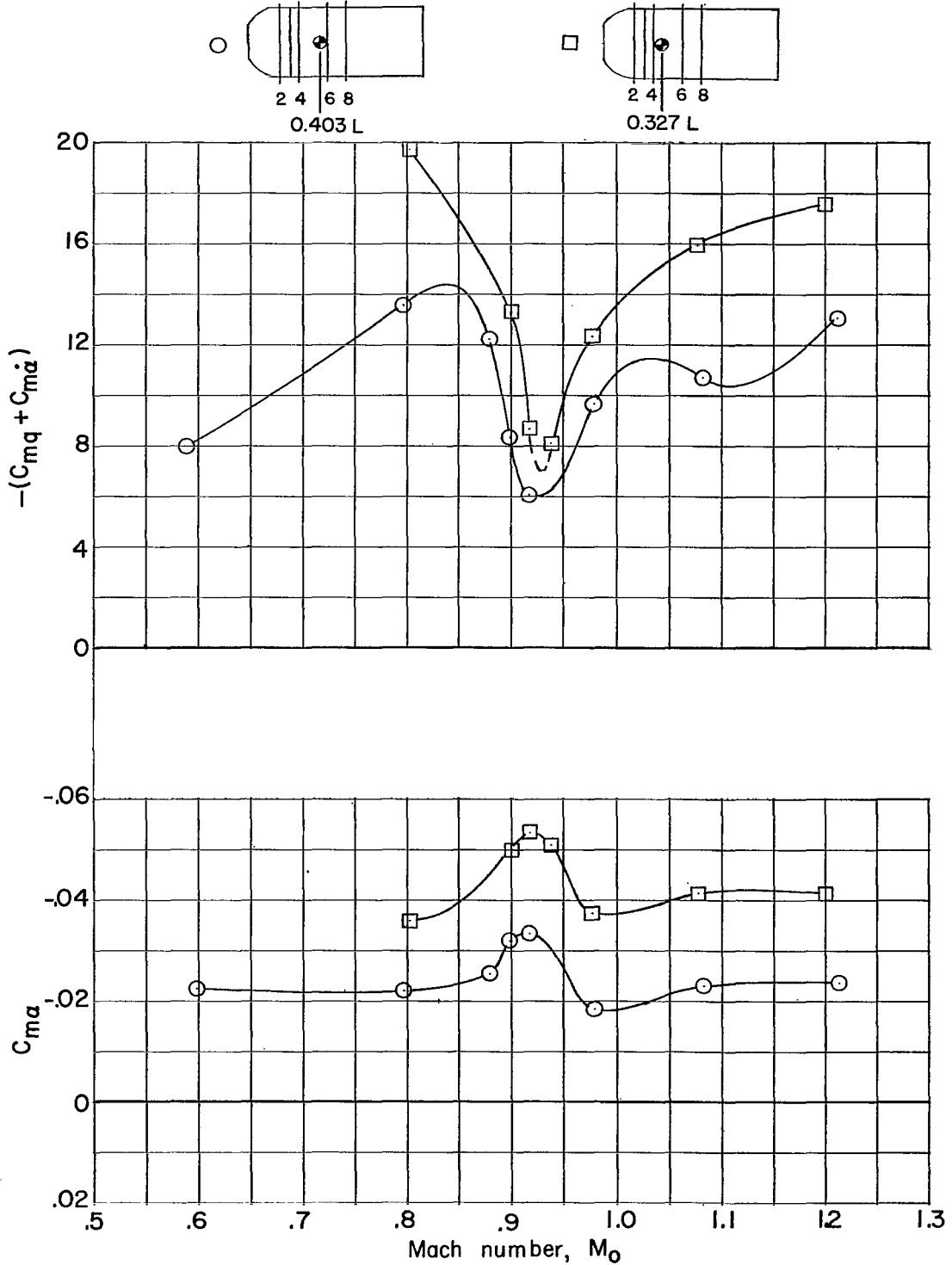


Figure 16.- The effects of a change in center-of-gravity position on the longitudinal stability of the TX-21 with nose A and the 6°-14° fins.

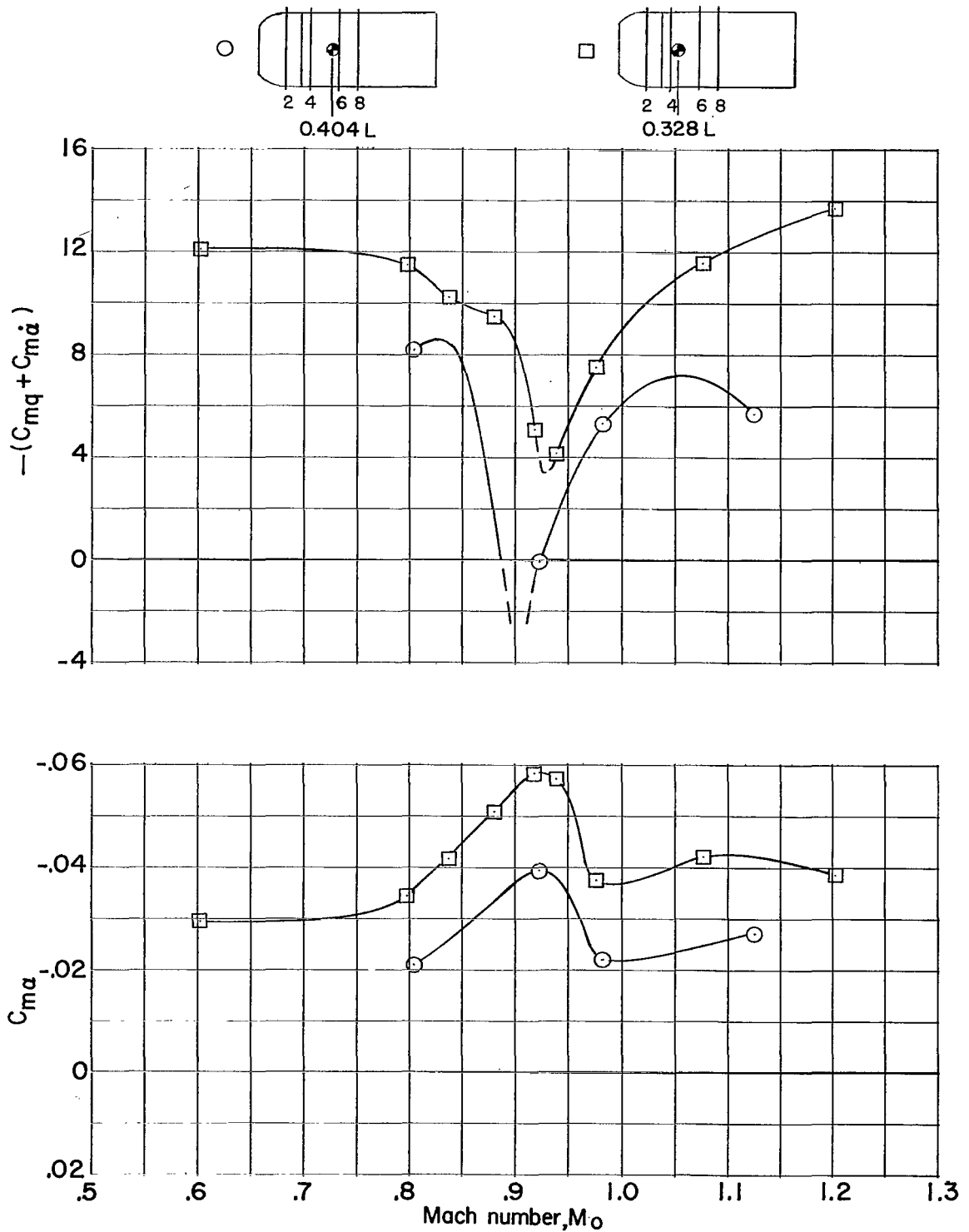


Figure 17.- The effects of a change in center-of-gravity position on the longitudinal stability of the TX-21 with nose B and the 6°-14° fins.



○ 0.6 atm
□ 1.0 atm

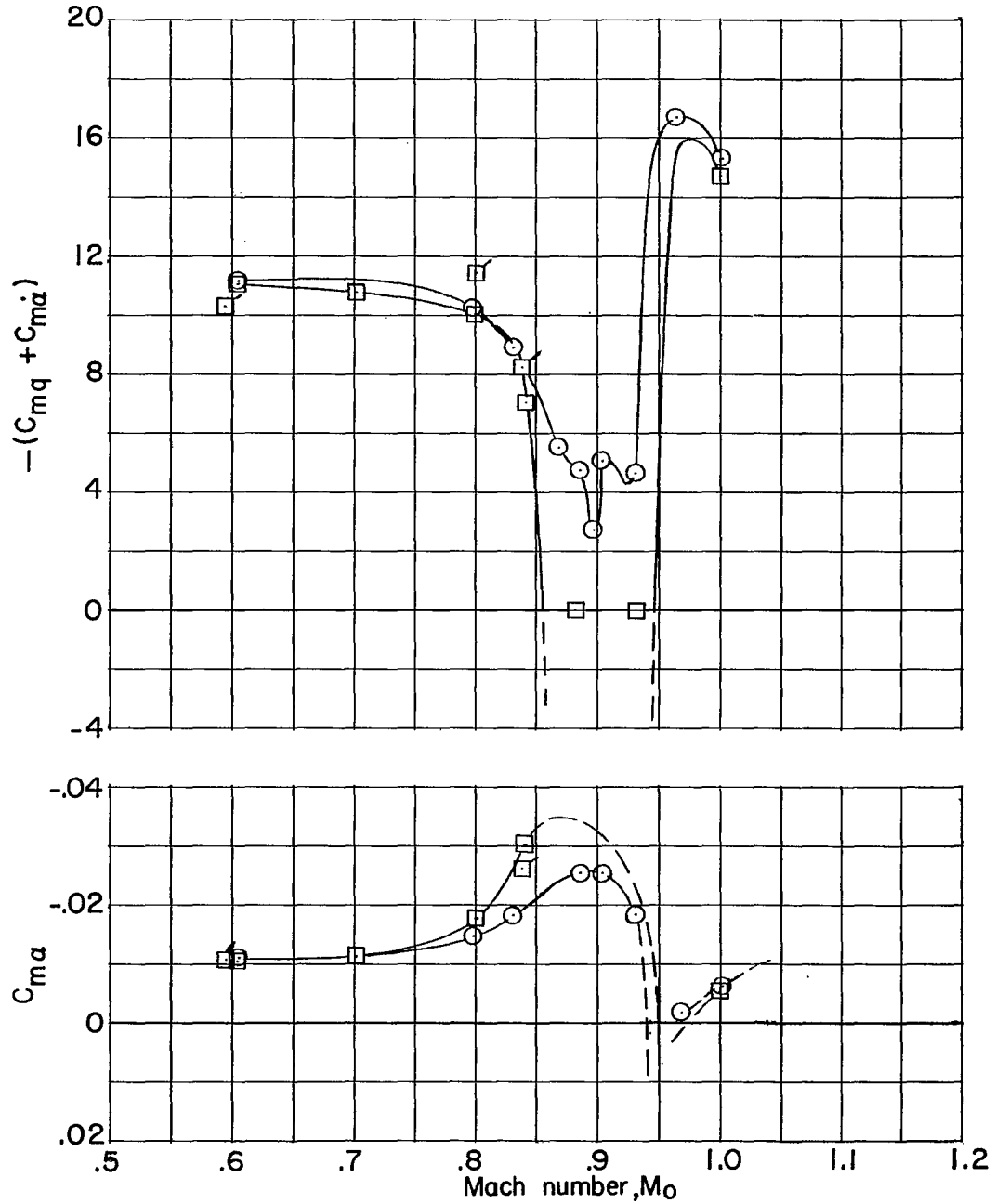


Figure 18.- The effects of a change in stagnation pressure on the longitudinal stability of a clean configuration of the TX-21 with nose A and the 6°-14° fins.

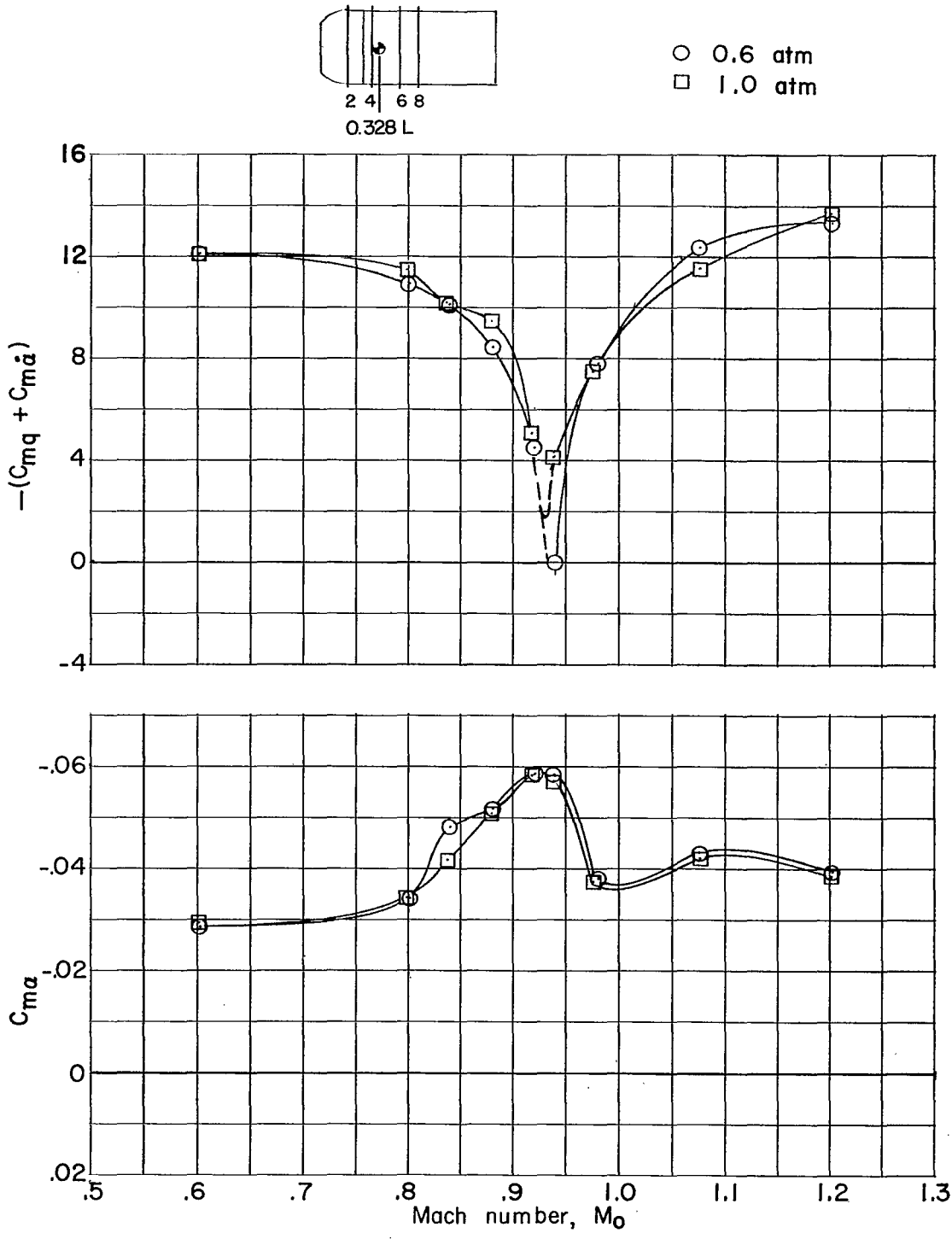


Figure 19.- The effects of a change in stagnation pressure on the longitudinal stability of a banded configuration of the TX-21 with nose B and the 6°-14° fins.

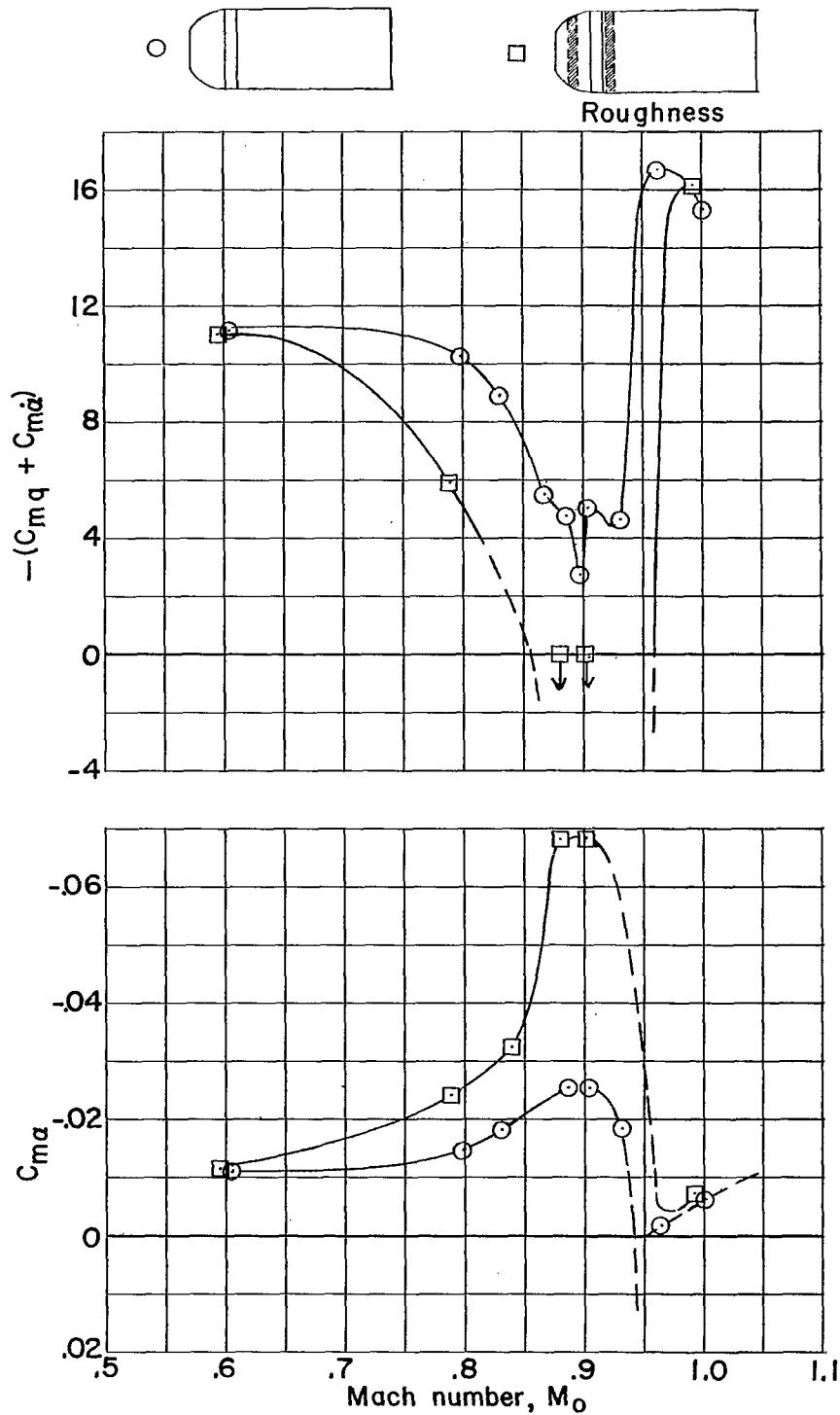


Figure 20.- The effects of artificial roughness on the longitudinal stability of the TX-21 with nose A and the 6° - 14° fins at 0.6 atmosphere.

NASA Technical Library



3 1176 01438 6800

